IMPROVEMENT OF VIBRATION TEST - CONVERTING A SINGLE-AXIS VIBRATION TABLE INTO A TWO-AXIS TABLE

By

Yanzhe Wu

A THESIS

Submitted to
Michigan State University
in partial fulfillment of the requirements
for the degree of

Packaging – Master of Science

2016

ABSTRACT

IMPROVEMENT OF VIBRATION TEST - CONVERTING A SINGLE-AXIS VIBRATION TABLE INTO A TWO-AXIS TABLE

By

Yanzhe Wu

An increasing number of companies find that their products pass standard vibration tests but are damaged during transportation. The main reason for this is that the vibration tables used in these tests only move up and down, meaning they lack 5 of the 6 motions that occur in real transportation. Converting a single-axis table to a six-axis table is almost impossible to do. Therefore this research investigated an alternative solution to this problem by adding the second most severe motion, roll. The concept of adding roll to a vertical shaker was to place a rocking platform on the table to act as the new vibration plane. When the table is vibrating, the platform will move both up and down and rock. Theoretically, the rocking motion can be made to match that in a trailer by adjusting two variables of the platform system. The theoretical RMS G could not be verified using test results due to unwanted noise and vibrations produced by the platform flexing and the axle wobbling. However, good agreement between the predicted and experimental rocking natural frequency showed that the concept has some merit. After fixing the problems with the structure of the platform, the next step for this research will be to test actual packages on a trailer and on the platform.

ACKNOWLEDGMENTS

First and foremost I wish to express my gratitude to my thesis advisor, Dr. Gary Burgess, who is the one professor who truly made a difference in my life. He is very knowledgeable and experienced in packaging distribution; I would not have considered a graduate research in this area if he were not my major professor. He provided me with direction, technical support and became more of a mentor and friend than a professor. He helped me come up with the thesis topic, build the test prototype and figure out the problem I met in the research and the writing. Dr. Burgess is very good at inspiring and guiding people to think on their own, my critical and analytical thinking was developed during this process.

I would also like to thank the other members of my committee, Dr. Robert Clarke and Dr. Brian Feeny. They shared their thoughts and concerns at the beginning and pointed out the shortcoming of the thesis and the better direction to revise it at the end. I am gratefully indebted to their very valuable comments on this research.

Finally, I must express my very profound gratitude to my beloved grandparents (Jiqin Chen and Zhenmei Wang), parents (Qikun Wu and Dongmei Chen) and my dear friends (Zhengyang Yang and Jin Zhang) for providing me with unfailing support and continuous encouragement throughout my years of study and through the process of researching and writing this thesis. I would not make it complete without them.

TABLE OF CONTENTS

LIST OF TABLES

LIST OF FIGURES

KEY TO SYMBOLS

a	Distance from the axle of the platform to the spring (in)
A and B	Constants
c	Viscous damping coefficient for the platform system (lb-sec/in)
C_1, C_2 and C_3	Constants that depend on the platform construction
C_4 to C_9	Arbitrary constants
d	Horizontal distance from the axle of the platform to the system's center of gravity (in)
D	Distance from the trailer centerline to the floor position to be simulated (in)
f_θ	Rocking natural frequency of the platform (Hz)
F	Upward force exerted by the axle on the platform (lbs.)
g	Acceleration of gravity (386.4 in/sec^2)
G	Acceleration (g's)
G_x	Lateral acceleration (g's)
G_{xp}	Lateral acceleration of the platform (g's)
G_{xt}	Lateral acceleration on the centerline of the trailer floor (g's)
G_z	Vertical acceleration (g's)
G_{zp}	Vertical acceleration of the trailer floor at the position to be simulated, or vertical acceleration of the platform axle (g's)
G_{zt}	Vertical acceleration on the centerline of the trailer floor (g's)
H_p	Height of the SAVER above the platform (in)

H_t	Height of the SAVER above the trailer floor (in)
I_{CG}	System moment of inertia, an axis through the center of gravity on the platform system (lb. in^2)
k	Spring constant on one side of the platform (lb/in)
mg	Combined weight of mass, platform and test package (lbs.)
M_m	Weight of the mass on the platform (lbs.)
θ	Counterclockwise rotation of the platform from the static position (rad)
θ_{st}	Angle of rotation of the platform from the horizontal plane at rest (rad)
θ_0	Starting value for the angle of the platform relative to the static position when vibrating (rad)
$\dot{\theta}$	Angular velocity of the platform (rad/s)
$\dot{\theta}_0$	Starting value for the angular velocity of the platform when vibrating (rad/s)
$\ddot{\theta}$	Angular acceleration of the platform (rad/s^2)
$\ddot{\theta}_t$	Angular acceleration of the trailer floor (rad/s^2)
N	Total number of samples
P	Position on the trailer floor to be simulated
R	Damping ratio
$RMS\ G_{x,p}$	Lateral RMS G of the platform (g's)
$RMS\ G_{x,t}$	Lateral RMS G on the centerline of the trailer floor (g's)
$RMS\ G_{z,p}$	Vertical RMS G of the trailer floor at position P (G's)
$RMS\ G_{z,t}$	Vertical RMS G on the centerline of the trailer floor (g's)
X_m	Distance from the platform axle to the mass (in)

t	Time (msec)
Δ	Difference between $RMS\ G_{z,t}$ and $RMS\ G_{z,p}$ (g's)
Δt	Time interval (msec)
ω	Angular frequency (Hz)

KEY TO ABBREVIATIONS

PSD	Power Spectral Density
ASTM	American Society of the International Association for Testing and Materials
MAST	Multi-Axis Simulation Table
RMS G	Root Mean Square G
OD	Outside Diameter
ID	Inside Diameter
TTV	Touch Test Vibration Controller
TP3	Test Partner®
CG	Center of Gravity
std.dev	Standard deviation

CHAPTER 1 INTRODUCTION AND LITERATURE REVIEW

1.1. Vibration test

Mechanical vibrations and shocks that happen during transportation cause most of the damage to packages and products. In order to avoid insufficient or excessive packaging, a valid and economic testing method is necessary. The vibration test is the most common method used to simulate the transportation environment in labs.

The vibration test is performed with vibration tables. The most common vibration table is the single-axis shaker, which reproduces the most severe vibration - vertical motion. Test packages are mounted on the vibration table, which then moves only up and down. Figure 1 is an example of the single-axis vibration table (Lansmont, 2010).

Figure 1 Single-axis vibration table

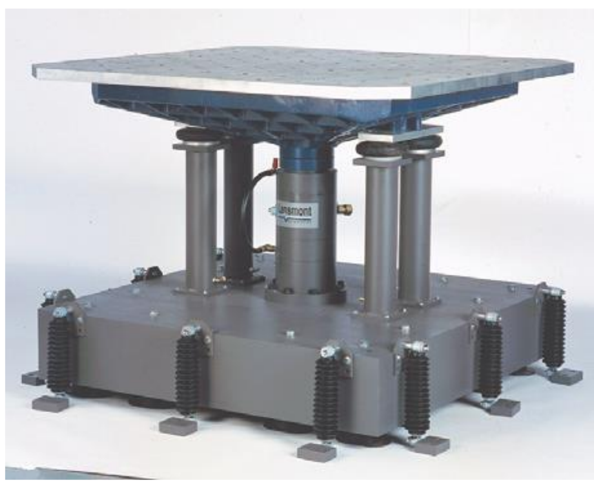

The vibration table is driven by a power spectral density (PSD) plot. This is a plot of power density versus frequency (see Figure 2 as an example). These power densities are related to accelerations collected by vibration recorders mounted on the floor of a truck trailer or railcar. The transportation environment is simulated in the lab by using the specific PSD plot with the same frequencies and power densities as those that were recorded. In order to simplify the procedure, the standard ASTM D4728 (ASTM, 2012) provides representative PSD plots that simulate typical random vibration environments. Figure 2 shows separate PSD plots for vertical motion, lateral (side-to-side) motion, and longitudinal (front to back) motion (Burgess, 2013). In the frequency range of interest (2-8 Hz), vertical vibration is normally 1 to 2 orders of magnitude higher than lateral and longitudinal vibrations. This is the main reason that vibration tables are constructed as single-axis shakers.

Figure 2 PSD plot for vertical, lateral and longitudinal vibrations of a trailer

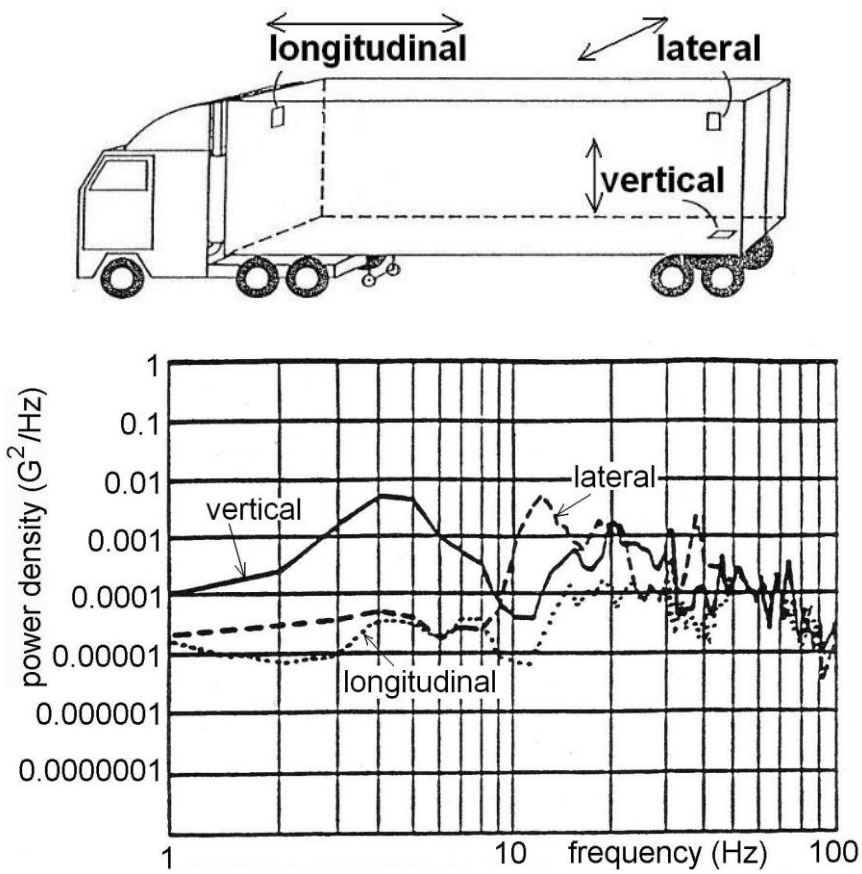

This research focused on reproducing road transportation, which means tractor trailers. According to the trailer's structure, there are three parts that vibrate at different frequencies. They are listed in Table 1.

Table 1 Different vibration parts of the trailer

Suspension	2 Hz (fully loaded) to 8 Hz (empty trailer)
Tires	15 Hz (low pressure) to 20 Hz (high pressure)
Floor	50 Hz (fully loaded) to 100 Hz (empty trailer)

1.2. Problems with the vibration test

An increasing number of companies find that their products pass the standard vibration test but are damaged during transportation. The images shown in Figure 3 are examples (D. Leinberger/ABF Freight, e-mail, 2010). As the vertical vibration cannot cause this damage, these two pallet loads should have experienced large lateral displacements.

Figure 3 Stacked bags after truck transportation

In order to solve this problem, it is necessary to figure out all of the movements that occur to a trailer during transportation. As shown in Figure 4, the trailer can move in 3 linear directions and rotate about 3 axes. The 3 linear movements are surge (front to back), sway (side to side) and heave (up and down). These are the same as the longitudinal, lateral and vertical directions in Figure 2. They happen when trailers change speed, change lanes and go over bumps in the road, respectively. The 3 rotations are roll (rotation about surge axis), pitch (rotation about sway axis) and yaw (rotation about heave axis). Roll happens when the wheels on one side of the trailer go over potholes or bumps.

Figure 4 Movements of a trailer

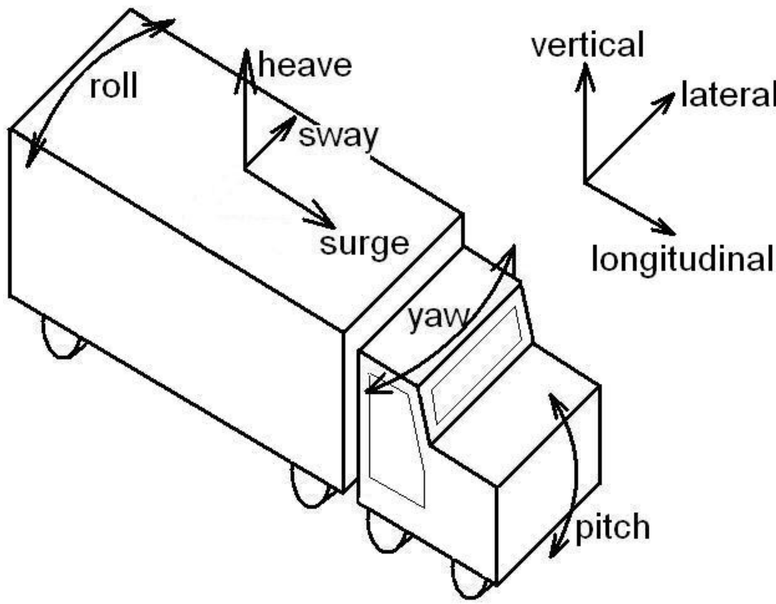

In Figure 3, the pallet-loads may have gone through roll and pitch motions. These are two movements that cannot be simulated on the vertical shaker. Real road transportation is a much more complex vibration environment. Current tables lack 5 of the 6 motions that occur in real transportation. This is why the test ASTM D4728 (ASTM, 2012) cannot be used to evaluate package integrity. Better vibration testing is badly needed.

1.3. Research on single-axis vibration versus multi-axis vibration

Singh (Singh, Antle, & Burgess, 1992) noticed that the lateral direction's power density level under 10 Hz could be as severe as that of vertical vibrations for heavily loaded truck trailers. It was because the rocking motion of the top load contributed to lateral vibration at low frequencies.

A vibration test for stacked corrugated packaging was conducted by Bernad in 2010. The result showed stackable packaging could resist more load from the vertical direction (compression) than other load directions (roll and pitch). Even though lateral and longitudinal excitations had less energy than vertical, they could contribute to sliding between layers in the stack and provoke the failure of the shipping unit (Bernad, Laspalas, González, Liarte, & Jiménez, 2010).

Bernad expanded the research to demonstrate the need for multi-axis testing in the lab. The test showed that the three linear motions combined only slightly increase the power density while the addition of rotational movements made the most significant change in the PSD plot. These energies are neglected in single-axis vibration test (Bernad, Laspalas, González, Núñez, & Buil, 2011).

Rouillard found that pitch and roll motions could be as damaging for shipments as vertical vibrations, even though they are relatively less severe (Rouillard, 2013). From experiments conducted to find the correlation between these three motions, Rouillard found that the type of road affects the overall intensity of the PSD plot, but not its shape. Also, the power density levels for all three motions generally increased linearly with vehicle speed.

Peterson used single-axis and multi-axis excitations to do time-to-failure tests on 10 digital clocks. The result showed six-degree of freedom motion caused failure in roughly half the time compared to vertical excitations alone. Additionally, the author noticed that if one clock was mounted in the center of the table and another was mounted slightly off to the side, the time to failure of the one off to the side was about two-thirds of the time to failure for the one in the center because one off to the side absorbed more energy from rotations (Peterson, 2013).

Lansmont provides a low-cost mechanical shaker for package testing (See Figure 5). The shaker can perform vertical-linear, circular-synchronous and 30° out-of-phase motions (refer to Figure 6). In the vertical direction, the shaker works like a single-axis vibration table without PSD control. When it does circular-synchronous motion, the table moves in small vertical circles at constant rotational speed. Consequently, the vertical and horizontal motions are sinusoidal. When the motion is 30° out-of-phase, the shaker simulates vertical, longitudinal and pitch movements at the same time (Lansmont, 2012).

Figure 5 Lansmont mechanical shakers

Figure 6 Circular-30° out-of-phase motion

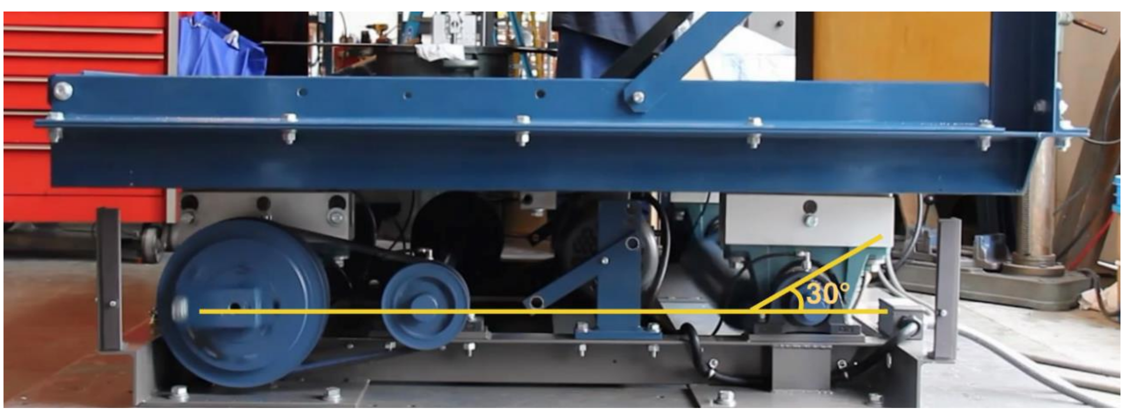

FedEx uses rotary vibration as one of its test procedures for packaged products weighing up to 150 lbs. The rotary vibration tester works similar to Lansmont mechanical shaker using circular-synchronous motion (FedEx, 2011).

A six degree of freedom multi-axis simulation table (MAST) is the one of the best simulators of the real environment (see Figure 7). The automotive industry was one of the first to employ this multi-axis vibration table. Figure 7 - 9 show a six-axis shaker used for automotive testing (Control Power-Reliance, personal communication, October 2013).

Figure 7 MAST being used to test finished cars for rattles and squeaks

Figure 8 Multi-axis table being used to test auto parts in racks

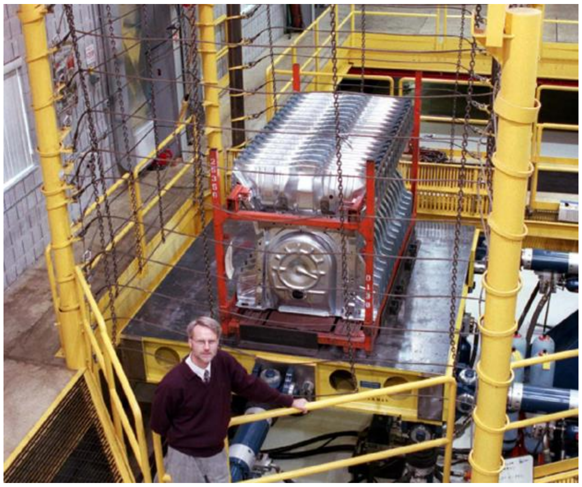

Figure 9 Six hydraulic pumps need to drive the table

Lansmont provides a multi-axis vibration test system, called the CUBE^{TM} (see Figure 10). It claims to be able to simulate real world 6-degree of freedom motion. The top mounting surface is 32 × 32 in (Lansmont, 2014). At the present time, the price of the CUBE^{TM} is about \$1,000,000 while their single-axis shaker (refer to Figure 1) is about \$200,000. Lansmont believes that the value of multi-degree of freedom vibration testing will increase significantly in the next several years, especially for testing pharmaceutical and electronic products (J. Breault/Lansmont, e-mail, September 2015).

Figure 10 Lansmont - CUBE^{TM} vibration tester

Lansmont conducted a test to verify the necessity of the multi-axis shaker. This experiment also showed how the truck really moves during transportation (Root, 2014). The truck was driven on California roads. Lansmont vibration recorder, the SAVER 9X30, was mounted on the trailer floor with two external triaxial accelerometers to record synchronous acceleration versus time measurements in 3 directions. At first, the CUBE™ vibration tester was driven with only vertical input. Even though the tester reproduced the vertical motion very well, the test item did not respond the same way on the trailer. Other inputs (pitch, roll and yaw) were then added to the CUBE™. The motion of the test item was finally consistent with what happened on the truck. It showed that only multi-axis tables like the CUBE™ could reproduce actual vibration.

1.4. Alternative solution – combining the 2 most important motions

High-technology always comes with a high price. In addition to the shaker, there are also maintenance and space costs. 6-axis shakers usually require more lab space and more powerful drive mechanisms than the single-axis table. Therefore, these shakers are not used by most companies in the packaging industry at the present time.

Single-axis vibration tables are currently owned by a great many institutions and companies. This was not a small investment, even though the single-axis table is not nearly as expensive as a multi-axis shaker. What's more, current vibration test standards are all written for single-axis shakers.

What improvements can be made for these vertical vibration tables? If the existing single-axis shakers could be made to function like a multi-axis vibration table at low-cost, this problem would be solved. However, this is almost impossible to do using the current single-axis table. It is possible however to add one of the five remaining motions, roll.

A truck trailer's suspension system is either air-ride or leaf-spring. They can both be modeled as a spring system. The end view of the trailer is shown in Figure 11.

Figure 11 Simplified trailer suspension system

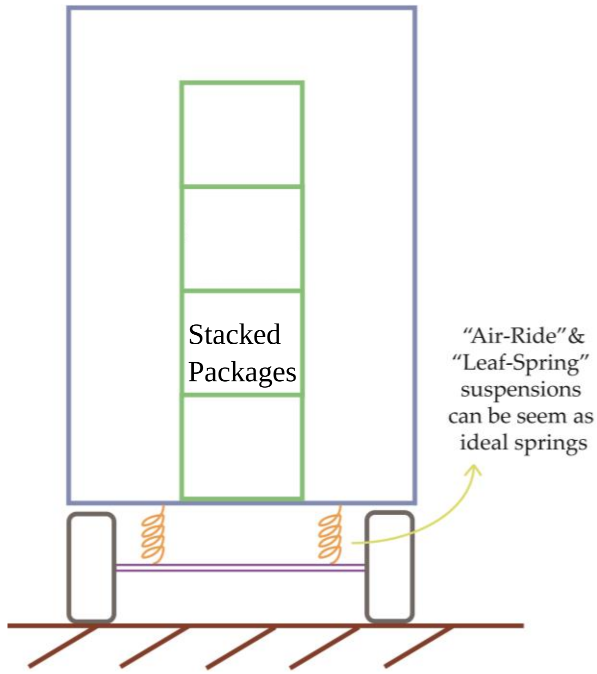

In addition to heave motion, roll is another motion that occurs all the time during transportation. Roll happens when the wheels on one side of the trailer go over potholes or bumps. Therefore, as long as the trailer is driving on an uneven road, there will be a roll motion. Uneven roads are what we have in the real world. Only when the wheels on both sides of the trailer hit a step bump at the same time, like raised pavement, will the trailers execute vertical motion. A comparison of real road conditions with road conditions that current vibration tables simulate is shown in Figure 12.

Figure 12 Uneven road causes roll vs. single-axis vibration table

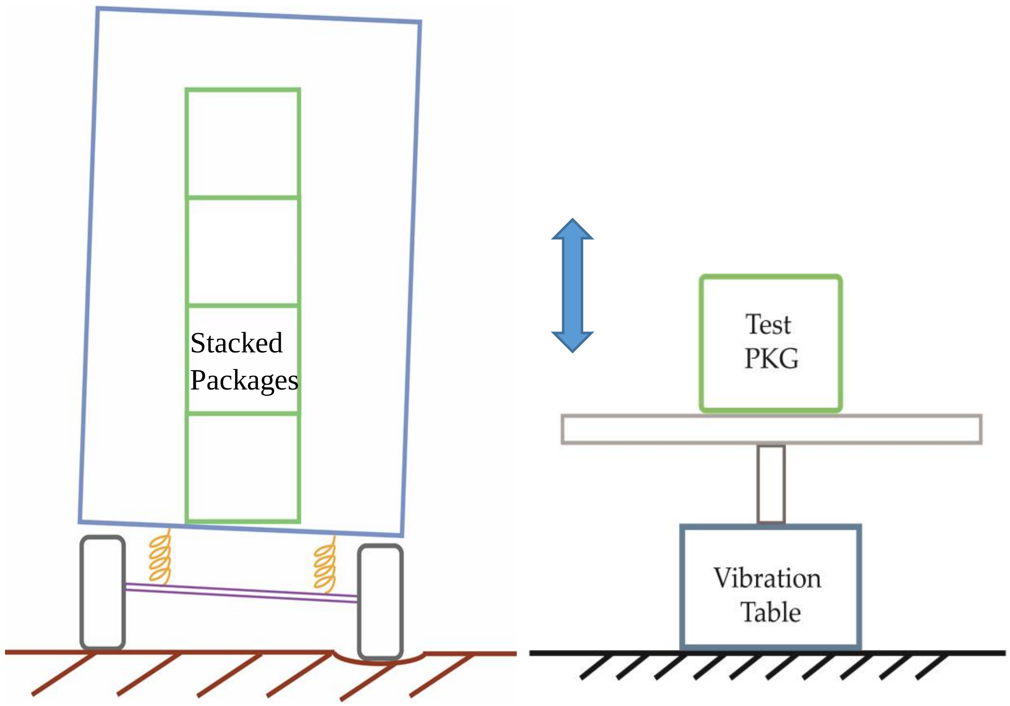

When trailers drive over uneven roads, the axle is always inclined. This excitation is transferred to the trailer body by the suspension system and causes side to side movement of packages, especially tall stacks. For stacked packages, roll may be the primary risk. Packages are designed to support top load, so they have better resistance to compression than bending. Misalignment between stacked packages and layers could amplify the problem (Bernad et al., 2011).

The remaining movements, surge, sway and yaw, only occur when the trailer changes speed, changes lanes and makes turns. These three excitations are long duration events that can last for several seconds. They require large displacements relative to vertical and roll motions that the vibration table would have to reproduce. Therefore, they cannot be replicated by single-axis shakers in the lab. The same is true for 6-axis shakers.

Roll and pitch are the only two motions that can be added to the single-axis vibration table. Pitch angles are much smaller than roll angles, so adding the second most severe motion, roll, to a single-axis vibration table was investigated in this research as an alternative to a six-axis shaker.

1.5. Objective and hypotheses

The goal of this research was to reproduce the rolling motion of the trailer using an add-on to a single-axis vibration table. This add-on is a rocking platform.

In order to achieve this goal in a more controlled way, a prediction model was developed. This model was used to predict the rocking natural frequency of the rocking platform (f_θ, where θ is the angle of rotation from the horizontal plane) and the overall severity of the vibration – Root Mean Square G (RMS G). A trustworthy prediction model should show good agreements between the predicted values and experimental results. Therefore, the hypotheses of this research were that predicted f_θ and RMS G would be consistent with experimental results.

CHAPTER 2 METHODS AND MATERIALS

2.1. Vibration table simulation

The original concept of adding rocking motion to a vertical shaker was to place a rocking platform on the table to act as the new vibration plane. A steel pipe is used as the axle. It passes through the platform and allows it to rotate. A spring is used to support the other side (refer to Figure 11). When the table is vibrating, the platform will heave and rock at the same time. Several prototypes of the platform have been explored based on this initial concept.

a. The initial concept, shown in Figure 13, will be called version 1 (k is the spring constant). This system has a vertical frequency, which can be adjusted to simulate real transportation. The rocking frequency and amplitude can be set to match target values by adjusting the spring stiffness. Because the package is not directly over the pivot, the vertical motion will not be the same as that of the vibration table. In addition, the vertical amplitude could be magnified. This will require the PSD plot that drives the table to be modified. Additionally, the spring end might lift off the table, especially if resonance is created.

Figure 13 Initial idea (version 1)

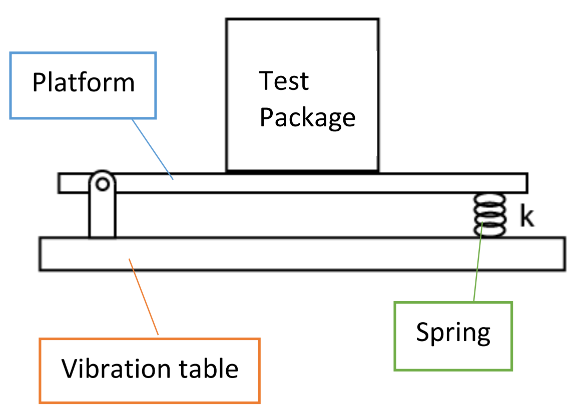

b. Figure 14 shows two more prototypes based on the initial concept. Both will be called version 2. Since the test package is over the pivot, the vertical frequency and amplitude of the package will exactly match the vertical frequency and amplitude of the vibration table. This is what we want because the table is being driven by a PSD plot that is supposed to recreate the vertical vibration of the floor of a truck trailer. But both of these designs have problems:

   For the platform with springs (left), the rocking frequency and amplitude could be matched to that of the trailer floor by adjusting the spring stiffness. However, the spring end might lift off the floor, which poses a safety risk.

   For the platform with a second axle (right), the rocking amplitude could be matched to that of the trailer floor by adjusting the position of this axle. For both, the rocking frequency of the platform is related to the vertical frequency of the vibration table while they should be independent.

Figure 14 Alternative platforms (version 2)

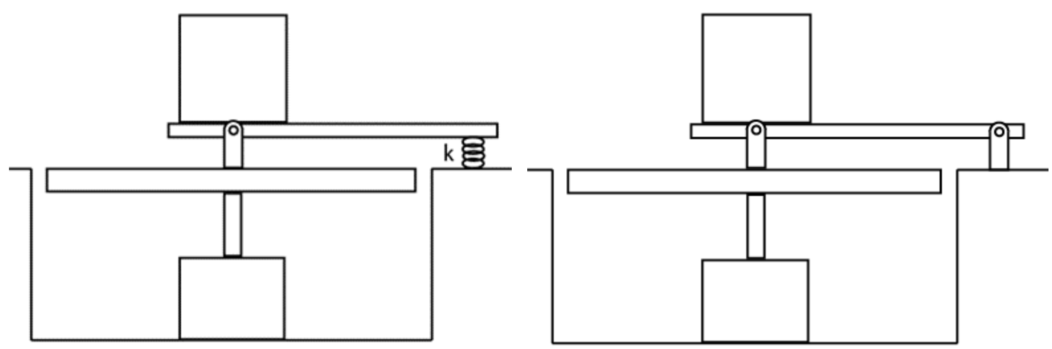

c. The prototype in Figure 15, called version 3, keeps all of the virtues of version 2 but mitigates their faults. Version 3 can simulate the rocking frequency and amplitude by adjusting the different spring stiffnesses on each side. Additionally, the rocking amplitude is self-limiting, which ensures that the platform will not go into resonance. This is closer to a real trailer. However, since the spring stiffnesses on each side are different, the platform might not respond the same as the floor of the trailer, where the stiffnesses are the same on each side.

Figure 15 Better platform (version 3)

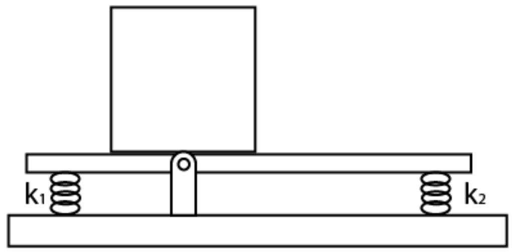

d. After further refining, the final prototype (version 4) of the platform is shown in Figure 16. The axle passes through the center of the platform and springs with the same spring constant are used on both sides. In addition to imitating the vertical motion, rocking motion is introduced by adding a solid mass on one side. When the table is vibrating, the platform will move up and down in synch with it and rotate, like a seesaw. This prototype can also account for the crown in the road by initially tilting the platform. Additionally, if the springs are replaced by blocks, the platform will revert back to a regular single-axis shaker (Figure 16, right).

Figure 16 Final prototype of the platform (version 4)

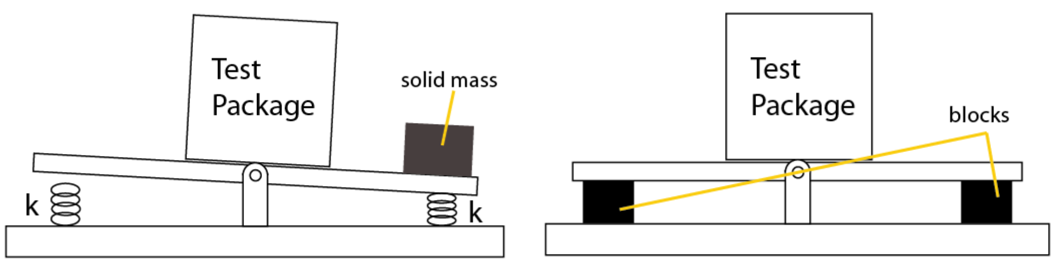

2.2. Materials

a. The platform was made from ¾’’ plywood. An “A-frame” was attached to the platform to provide a mounting surface for a vibration recorder, the SAVER. The actual platform is shown in Figure 17.

Figure 17 The actual platform

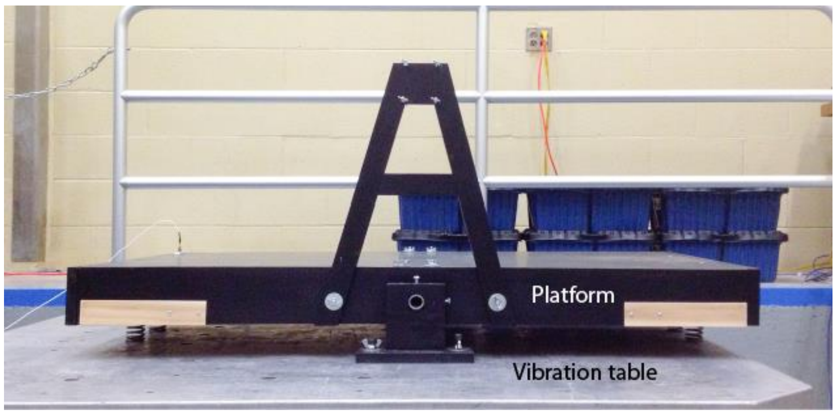

Weight: 31.33 lbs.

Deck length x width x thickness: 47.25’’ × 27.75’’ × 0.75’’

Supporting frame underneath (thickness x width x length):

5 ribs along the length: 0.75’’ × 3.5’’ × 47.25 ’’

8 ribs: 0.75’’ × 3.5’’ × 6’’

Two end pieces that can be removed to install up to 4 springs in parallel on each end (thickness x width x length): 0.75’’ × 4.25’’ × 27.75’’

b. Axle

Weight: 6.67 lbs.

Steel pipe: 32’’ Long; 1.0625’’ Outside Diameter (OD) and 0.8125’’ Inside Diameter (ID)

c. Springs (see Figure 18)

Compression Spring - P/N C48-187-192 (W.B. Jones Spring Co.)

1.470 OD, 0.187 music wire, 6-inch overall length

Spring constant (k) – 60 lbs. /in.

Figure 18 Specifications for the spring

Part Number	C48-187-192
Outside Diameter (in.)	1.470
Inside Diamter (in.)	1.096
Overall Length (in.)	6.000
Wire Diameter (in.)	0.187
Rate (lbs./in.)	60.00
Load (lbs.)	151.8
Deflection at Load (in.)	2.53
Total # of Coils	15.9
Active # of Coils	13.9
Solid Height (in.)	2.968
Pitch (in.)	0.406
Space between the Coils (in.)	0.219
Ends	CLOSED AND GROUND
Material	MUSIC WIRE
Finish	PLAIN

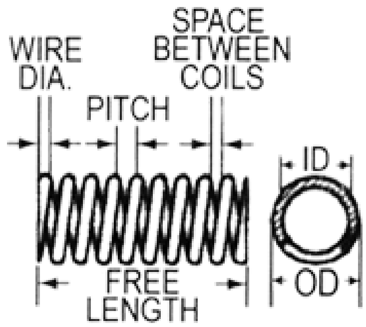

d. Bearings

Two wooden blocks with square holes for the axle.

Two screws in each block, one horizontal and one vertical, to adjust the position of the axle in the holes so that it doesn't wobble too much during vibration.

e. Steel Masses

Different weights were used to get the platform rocking. Their specifications are shown in Table 2.

Table 2 Steel Masses

Number	Weight (lbs.)	Dimensions (length x width x thickness)
5	5	6'' × 6'' × 0.5''
1	12.8	7.5'' × 6'' × 1''
2	32	7.5'' × 6'' × 2.5''

f. Vibration system

Lansmont vertical vibration table - Model 7000 and program TTV (TouchTest Vibration Controller)

g. Vibration recorder

Lansmont SAVER 3X 90 and program SaverXWare.

h. External accelerometer

Kistler 10 mV/g single-axis piezoelectric accelerometer and program TestPartner® (TP3)

2.3. Matching the trailer motion

Since the test package is placed directly over the axle, its vertical motion is the same as that of the vibration table. Therefore, how to reproduce the rocking motion was the main objective that needed to be researched. Rocking frequency and rocking amplitude are two independent parameters that need to be considered. The natural frequency in the rocking mode can be determined from either a bump test or a frequency sweep looking for resonance.

For the bump test, an accelerometer was mounted on the platform and connected to a computer with TestPartner® (TP3) (see Figure 19).

Figure 19 Platform in the bump test

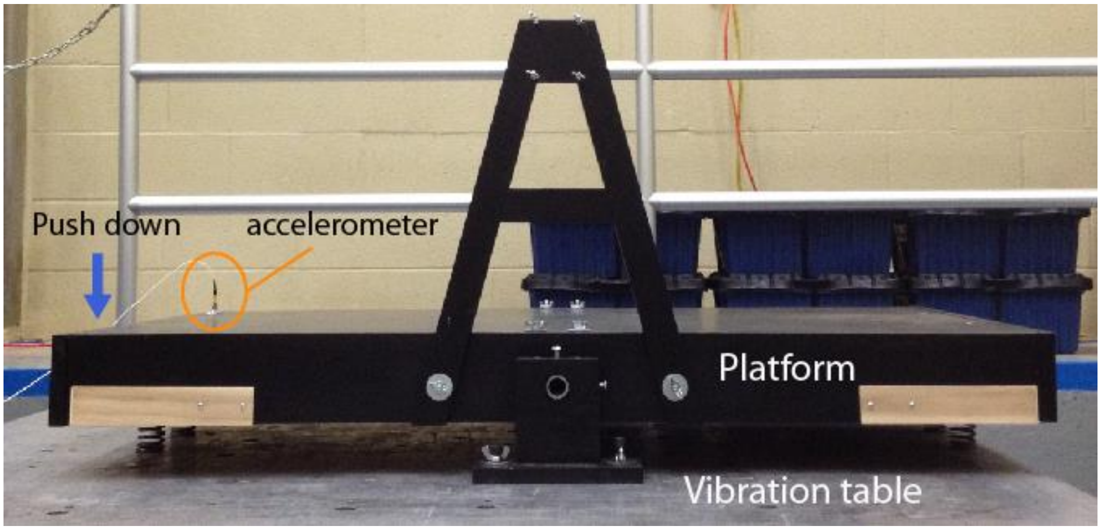

After the platform was pushed down and released, TP3 recorded the vibration. It showed an exponential decay curve as in Figure 20. The time interval between peaks, such as t_1 to t_2, is the period of vibration. The reciprocal of the period is the rocking frequency: $f_\theta = \frac{1}{t_2 - t_1}$

Figure 20 Decaying sine wave from the bump test

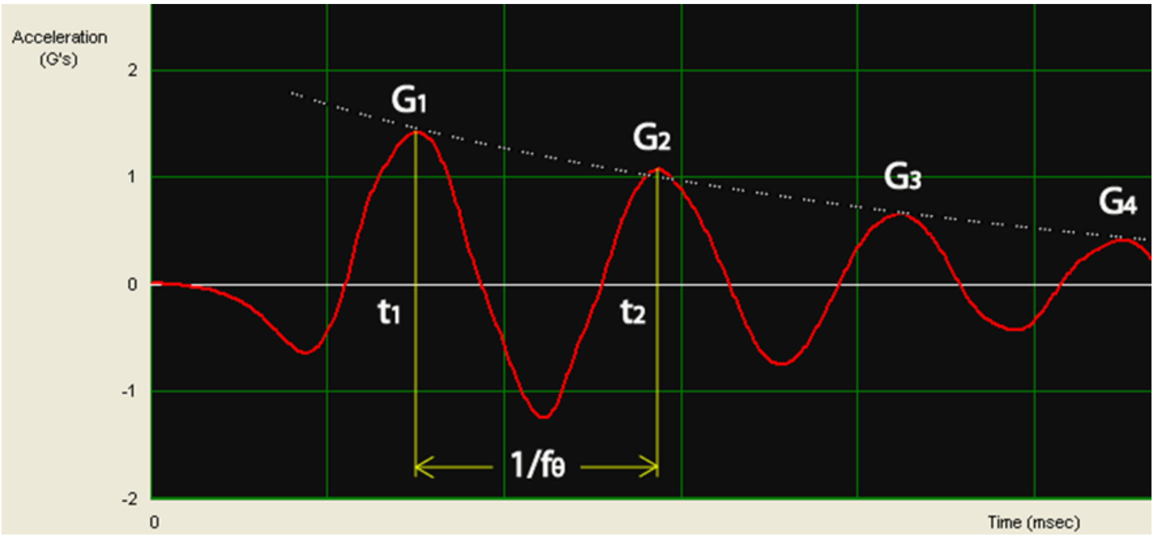

For a damped spring-mass system responding to a bump test, Equation (1) describes the behavior in Figure 20 (Shabana, 1995):

$$\ddot{\theta}+C_1\dot{\theta}+C_2\theta=0 \tag{1}$$

The solution to Equation (1) is

$$\theta=e^{\frac{-C_1 t}{2}}\left[\mathrm{A}\sin\left(t\sqrt{C_2-\frac{C_1^{\,2}}{4}}\right)+\mathrm{B}\cos\left(t\sqrt{C_2-\frac{C_1^{\,2}}{4}}\right)\right] \tag{2}$$

where A and B are constants. The natural frequency is:

$$f_\theta=\frac{1}{2\pi}\sqrt{C_2}\cdot\sqrt{1-\frac{C_1^{\,2}}{4C_2}} \tag{3}$$

and the damping ratio is:

$$R=\frac{C_1}{2\sqrt{C_2}} \quad \left(0<R<1\right) \tag{4}$$

The constants C_1 and C_2 in Equation (1) are related to the G's in Figure 20 by

$$C_1=\frac{2f_\theta}{N-1}ln\frac{G_1}{G_N} \tag{5}$$

$$C_2=\left(2\pi f_\theta\right)^2+\frac{C_1^{\,2}}{4} \tag{6}$$

where the accelerations G_1 and G_N are the first and last peaks at times t_1 and t_N.

The sweep test is another way to find the natural frequency. It uses the vibration table. The standard procedure is ASTM D999 (ASTM, 2015). The table is driven so that it moves up and down sinusoidally, slowly increasing the frequency from 3 Hz to 100 Hz. The natural frequency can be determined by observing the platform movement during the sweep test. Maximum amplitude can be identified by attaching an accelerometer to the platform. When the platform rocks wildly, it has reached resonance. It resonates whenever the table frequency matches its natural frequency.

The resonant frequency recorded during the sweep test should match the result from the bump test. Nevertheless, both tests give a natural frequency, which need not be the same as the trailer's rocking frequency during transportation because this frequency depends on the spacing of bumps on the road and the truck trailer's speed. Rocking natural frequency is not a variable that will be targeted but is nevertheless important because it does enter into calculations later.

The other parameter, rocking amplitude, is the maximum angle that the platform achieves during vibration. It cannot be measured directly because the SAVER only measures linear accelerations in three perpendicular directions. However, by mounting the SAVER above the platform, the horizontal acceleration that it measures during rocking can be related to angular acceleration. Angular acceleration can then be used to determine the rocking amplitude.

Since vibration in transit is normally random motion, rocking motion is also. Therefore, the RMS G (Root-Mean-Square G), which is a quantity that is measured by the SAVER, will be targeted. This is used to represent the overall severity of the motion. The goal will be to match this with what the trailer does.

Figure 21 shows a portion of a random vibration signal. The dots are acceleration samples recorded by the SAVER. The average of the recorded accelerations in Figure 21 will be zero because there are as many positive accelerations as negative ones. Positive accelerations result from the trailer floor moving up and negative accelerations from it moving down. The standard deviation, which is a measure of the variation in G values around the mean, is not zero. If N is the number of samples, the standard deviation or $RMS\ G$ in the x (lateral) direction is:

$$std.dev. = RMS\ G = \sqrt{\frac{\left(G_{x1}{}^{2} + G_{x2}{}^{2} + G_{x3}{}^{2} ... + G_{xN}{}^{2}\right)}{N}} \qquad (7)$$

Figure 21 Sampled accelerations

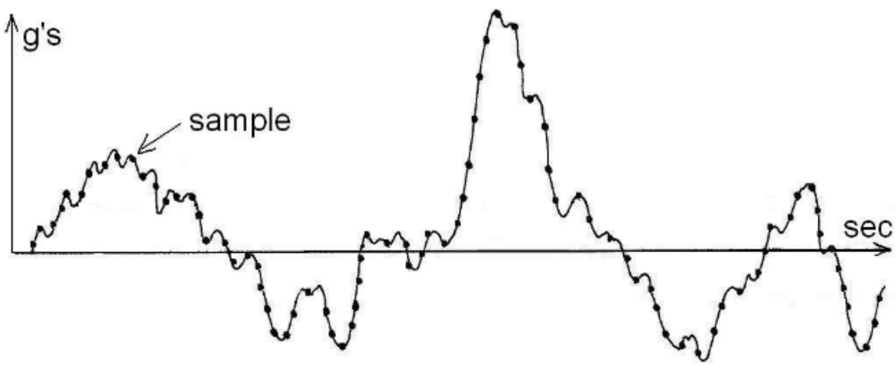

2.3.1. Target RMS G from trailer

Different locations on the trailer floor experience different RMS G's. The motion at the center, midway between walls, is usually the smoothest and near the walls, it is the roughest. The data recorded by the SAVER only represents the vibration where the SAVER is located. There are several steps needed to get the RMS G that the platform is supposed to simulate.

First, a lightweight beam is attached to the trailer floor as shown in Figure 22. The SAVER is mounted on it midway between walls at height H_t above the trailer floor. The SAVER's lateral (G_{xt}) and vertical (G_{zt}) accelerations are recorded at regular intervals, usually every 1 millisecond (refer to Figure 21). At every instant, the floor's angular acceleration ($\ddot{\theta}_t$) is related to the lateral acceleration experienced by the SAVER through:

$$\ddot{\theta}_t = -\frac{G_{xt}g}{H_t} \qquad (8)$$

where g is the acceleration due to gravity, 386.4 in/sec^2.

Figure 22 End view of a trailer with the SAVER on beam

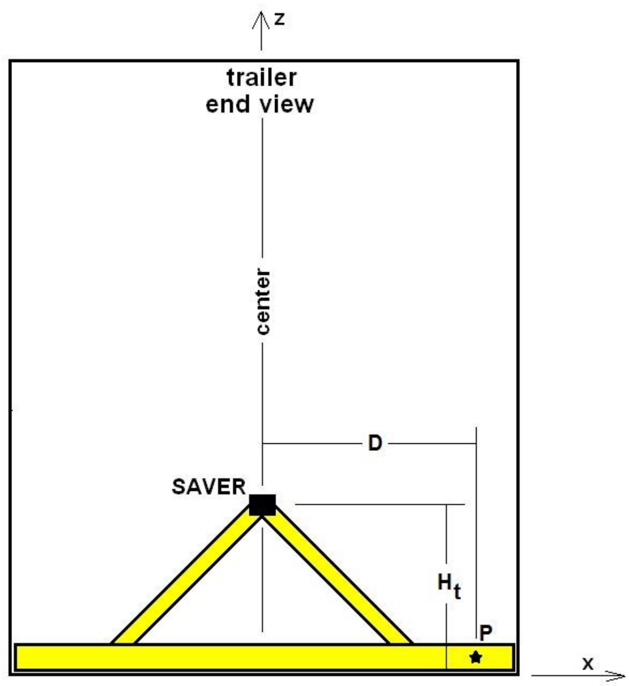

Next, if the motion at location P (Figure 22) on the trailer floor is to be simulated, where P is at distance D from the center line, the vertical acceleration (G_{zp}) at P will be:

$$G_{zp}g = G_{zt}g + D \cdot \ddot{\theta}_t \tag{9}$$

The platform should be set up to reproduce the angular and vertical accelerations in Equations (8) and (9) as closely as possible. Since it is highly unlikely that the platform will be able to reproduce them at every instant, only their RMS values will be targeted.

2.3.2. Simulated RMS G

The vertical motion of the trailer floor at position P is $G_{zp}\ vs.\ t$. This signal should be used to drive the vibration table. This makes the vertical acceleration of the platform directly over the axle the same as that of the trailer at P.

Vibration tables are driven by PSD plots. In order to get the PSD plot for location P, the recorded SAVER data needs to be processed. Substituting $\ddot{\theta}_t$ from Equation (8) into Equation (9) relates G_{zp} to the lateral and vertical accelerations recorded by the SAVER:

$$G_{zp} = G_{zt} - \frac{D}{H_t} \cdot G_{xt} \tag{10}$$

The vertical $RMS\ G_{z,p}$ at position P is related to trailer's vertical $RMS\ G_{z,t}$ and lateral $RMS\ G_{x,t}$ by:

$$\left(RMS\ G_{z,p}\right)^2 = \frac{\sum\left(G_{zt}{}^2 - \frac{2D}{H_t} G_{zt} \cdot G_{xt} + \frac{D^2}{H_t{}^2} G_{xt}{}^2\right)}{N}$$

where the sums are over the N samples taken at regular intervals. The middle sum is zero because G_{xt} and G_{zt} are independent random oscillations, both with means of zero. The first and third sums are related to the RMS G's recorded by the SAVER in the vertical and lateral directions.

$$\left(RMS\ G_{z,p}\right)^2 = \left(RMS\ G_{z,t}\right)^2 + \frac{D^2}{H_t{}^2}\left(RMS\ G_{x,t}\right)^2 \tag{11}$$

Since the RMS G squared is the area under its PSD plot, Figure 23 shows the meaning of Equation (11). In order to get the vertical PSD plot for position P, start with the vertical PSD plot the SAVER on beam provided and raise it up until the crosshatched area in Figure 23 is $\frac{D^2}{H_t{}^2}\left(RMS\ G_{x,t}\right)^2$. If the plot spans the usual frequency range of 3 Hz to 100 Hz, all power density (G^2/Hz) values are raised the same amount Δ, where $\Delta = \frac{\text{(crosshatched area)}}{100-3}$.

Figure 23 Relationship between vertical PSD plots for position P and center of trailer

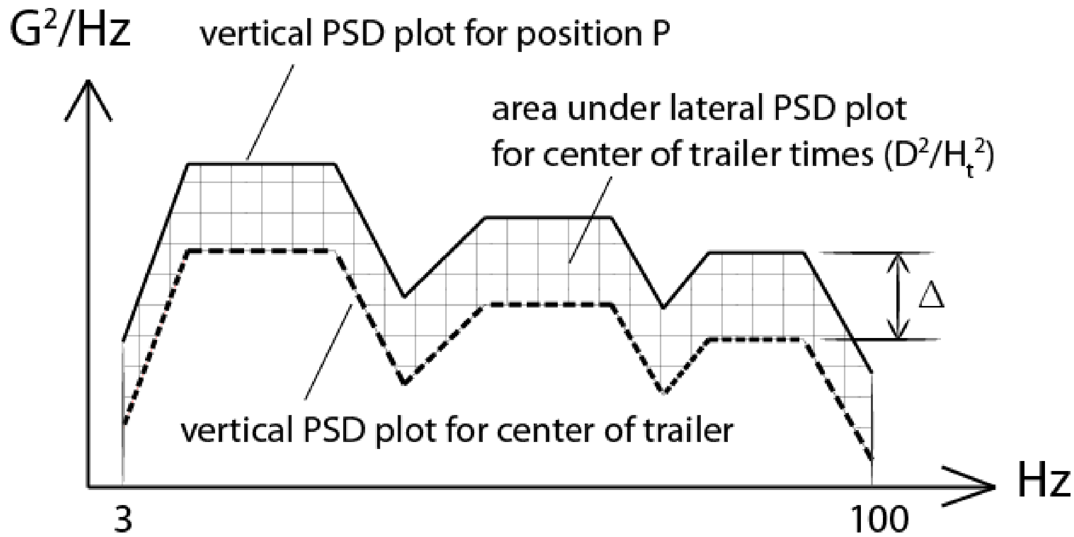

Now the rocking motion (angular acceleration) must be matched. Since the SAVER on the platform is mounted right over the axle to record the platform's lateral (G_{xp}) and vertical (G_{zp}) accelerations (Figure 24), the relationship between the lateral acceleration of the platform and its angular acceleration ($\ddot{\theta}$) is:

$$\ddot{\theta} = -\frac{G_{xp} g}{H_p} \tag{12}$$

Figure 24 Platform with SAVER 3X90 mounted on it

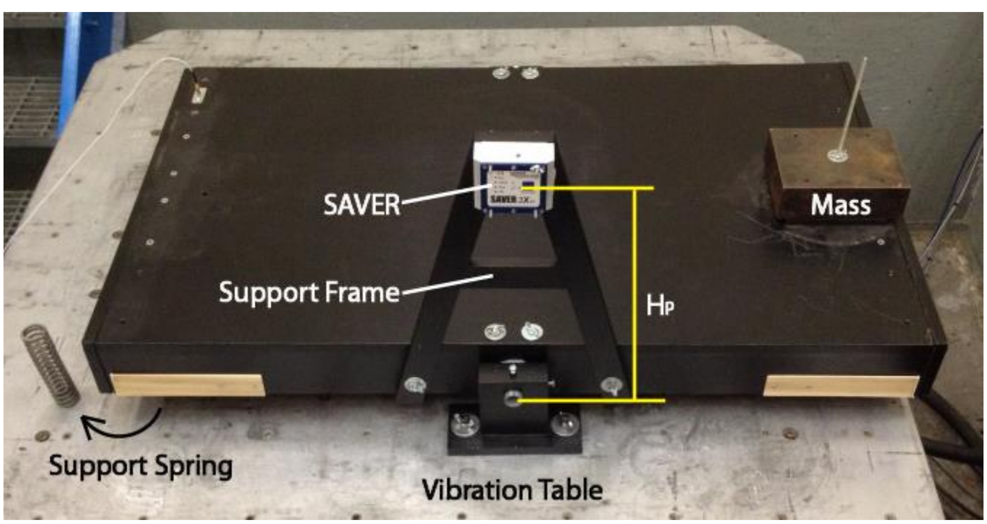

To make the platform move like the trailer, the angular accelerations ($\ddot{\theta}_t$ and $\ddot{\theta}$) should be the same:

$$-\frac{G_{xt}g}{H_t} = \ddot{\theta}_t = \ddot{\theta} = -\frac{G_{xp}g}{H_p} \qquad (13)$$

The platform's lateral acceleration at every instant should therefore be made to relate to the trailer's lateral acceleration at every instant by:

$$G_{xp} = \frac{H_p}{H_t} \cdot G_{xt} \qquad (14)$$

Trying to get the platform to do this at every instant will not be possible. Instead, Equation (14) will be satisfied in an RMS sense. In view of the definition of RMS G, the lateral RMS G's should therefore be related by:

$$RMS\ G_{x,p} = \frac{H_p}{H_t} \cdot RMS\ G_{x,t} \qquad (15)$$

The goal is therefore to make the lateral acceleration $RMS\ G_{x,p}$ measured by the SAVER on the platform be $\frac{H_p}{H_t}$ times the lateral acceleration $RMS\ G_{x,t}$ measured by the SAVER on the beam attached to the trailer floor. This can be done by adjusting the locations of the mass attached to the platform and the number of springs used. In order to prove this, the next section analyzes the theoretical motion of the platform.

2.3.3. Predicted motion

When the table is turned off, the platform is at rest (Figure 25). In this state, the platform rotates angle θ_{st} relative to the horizontal plane (st means static).

Figure 25 Initial state of the platform

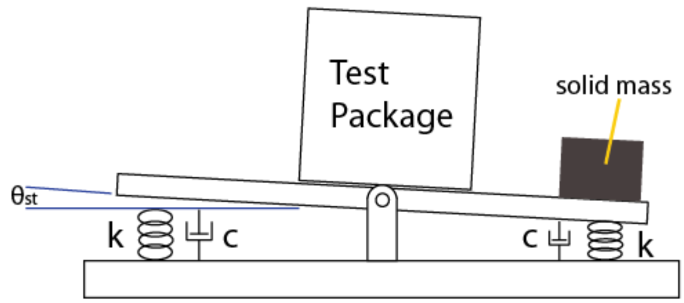

Since the platform is not moving, there is no damping force. The force diagram is shown in Figure 26.

Figure 26 Force diagram of the platform at rest

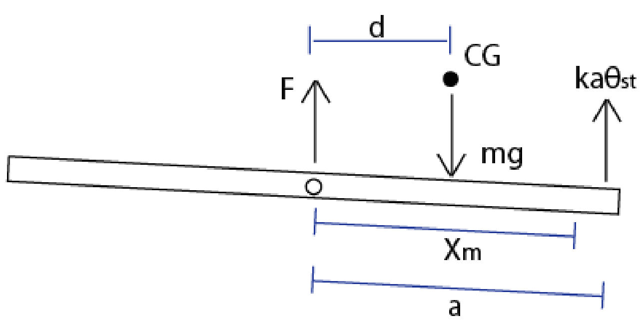

mg = combined weight of mass, platform and test package (lbs.)

F = support force exerted by axle (lbs.)

a = distance from the axle to the spring (in)

k = spring constant (lb/in)

X_m = distance from the axle to the mass (in)

d = horizontal distance from axle to system's center of gravity (CG)

In this figure, "k" represents the effective spring constant for the number of springs used (twice the "k" for one spring if two springs are used, three times the "k" for one if three are used, etc.). For the wooden platform that was built, "a" and "X_m" are fixed. It is expected that a commercial version of the platform will allow "a" and "X_m" to be varied.

The static rotation θ_{st} is obtained by summing moments about the axle:

$$ka\theta_{st} \cdot a = mg \cdot d \tag{16}$$

$$\theta_{st} = \frac{mg \cdot d}{ka^2} \tag{17}$$

When the vibration table is running, the platform is in a dynamic state. See the force diagram in Figure 27.

Figure 27 Force diagram of the platform in motion

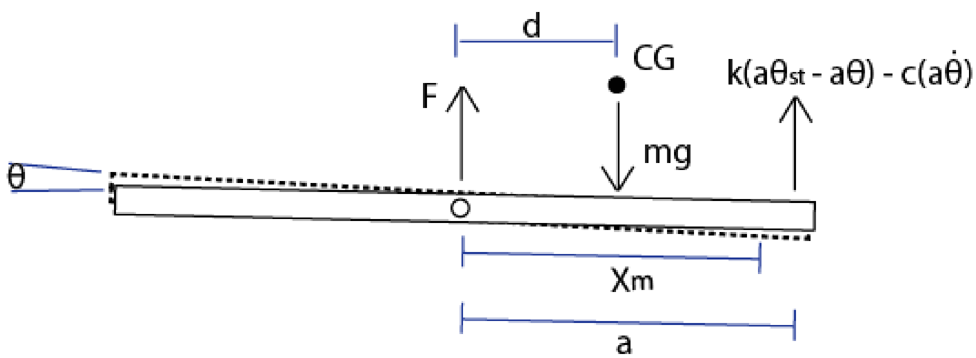

Summing vertical forces and moments about the center of gravity requires that:

$$F - mg + ka(\theta_{st} - \theta) - c \cdot a\dot{\theta} = m(G_{zp}g + d\ddot{\theta}) \tag{18}$$

$$-F \cdot d + ka(\theta_{st} - \theta)(a - d) - c \cdot a\dot{\theta}(a - d) = I_{CG} \cdot \ddot{\theta} \tag{19}$$

c = viscous damping coefficient for the system (lb-sec/in)

G_{zp} = known vertical acceleration of the axle

θ = counterclockwise rotation from the static position.

$\dot{\theta}$ = angular velocity of the platform

$\ddot{\theta}$ = angular acceleration of the platform

I_{CG} = system moment of inertia about an axis through the CG

Equation (18) was multiplied by d and added to Equation (19), producing Equation (20):

$$\ddot{\theta} + C_1 \cdot \dot{\theta} + C_2 \cdot \theta = C_3 \cdot G_{zp} g \tag{20}$$

$$C_1 = \frac{c \cdot a^2}{I_{CG} + m \cdot d^2} \tag{21}$$

$$C_2 = \frac{k \cdot a^2}{I_{CG} + m \cdot d^2} \tag{22}$$

$$C_3 = -\frac{m \cdot d}{I_{CG} + m \cdot d^2} \tag{23}$$

The homogeneous solution to differential Equation (20) is:

$$\theta = e^{\frac{-C_1 t}{2}} \left[C_4 \sin\left(\omega t\right) + C_5 \cos\left(\omega t\right) \right] \tag{24}$$

where C_4 and C_5 are arbitrary constants to be solved for later. The angular frequency is:

$$\omega = 2\pi f_\theta = \sqrt{C_2} \cdot \sqrt{1 - R^2} \tag{25}$$

where

$$R = \frac{C_1}{2\sqrt{C_2}} \quad \left(0 < R < 1\right)$$

Since the SAVER records vertical acceleration only at discrete times (every 1 millisecond), G_{zp} in Equation (20) is only known at discrete times. In order to solve Equation (20) accurately, the vertical acceleration is assumed to be piecewise linear between samples. For the first time interval ($0 \le t < \Delta t$), the vertical accelerations are shown in Figure 28. G_{z0} and G_{z1} are the sampled accelerations.

Figure 28 Piecewise linear vertical acceleration

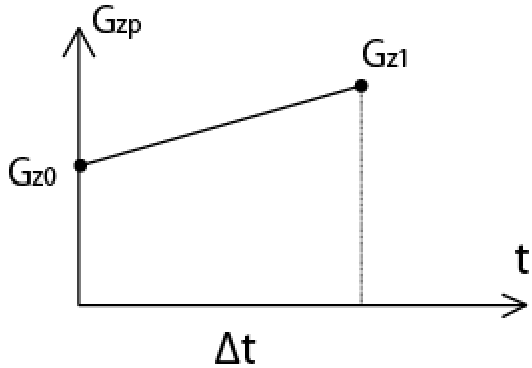

Within this segment, the vertical acceleration is represented by:

$$G_{zp} g = C_6 + C_7 t \tag{26}$$

where C_6 and C_7 were related to the sampled accelerations at the start and end of the interval:

$$C_6 = G_{z0} g \tag{27}$$

$$C_7 = \frac{G_{z1} - G_{z0}}{\Delta t} g \tag{28}$$

The particular solution to Equation (20) is:

$$\theta = C_8 + C_9 t \tag{29}$$

$$C_9 = \frac{C_3 C_7}{C_2} \tag{30}$$

$$C_8 = \frac{C_3 C_6 - C_1 C_9}{C_2} \tag{31}$$

The complete solution to the differential Equation (20) for $0 < t < \Delta t$ is the sum of Equation (24) and Equation (29):

$$\theta = e^{\frac{-C_1 t}{2}} \left[C_4 \sin(\omega t) + C_5 \cos(\omega t) \right] + C_8 + C_9 t \tag{32}$$

Taking the derivative of Equation (32) with respect to time gives:

$$\dot{\theta} = e^{\frac{-C_1 t}{2}} \left[-\left(\omega C_5 + \frac{C_1 C_4}{2} \right) \sin(\omega t) + \left(\omega C_4 - \frac{C_1 C_5}{2} \right) \cos(\omega t) \right] + C_9 \qquad (33)$$

In order to get C_4 and C_5, the starting values for the angle (θ) and angular velocity ($\dot{\theta}$) are needed.

At $t = 0$, if $\theta = \theta_0$,

$$C_5 = \theta_0 - C_8 \qquad (34)$$

At $t = 0$, if $\dot{\theta} = \dot{\theta}_0$,

$$C_4 = \frac{\dot{\theta}_0 + \frac{C_1 C_5}{2} - C_9}{\omega} \qquad (35)$$

This completes the solution to Equation (32). All of the C's are known. The angle and angular velocity at the end of the first interval are obtained using $t = \Delta t$ in Equations (32) and (33). These values are then used as starting values for the next interval ($\Delta t \le t < 2\Delta t$). In this way, the solution can be obtained in a recursive manner. The angular acceleration ($\ddot{\theta}$) and lateral acceleration (G_{xp}) at each instant are therefore also known from Equations (20) and (12). The $RMS\ G_{x,\,p}$ can therefore be obtained using the G_{xp} values calculated at each time step. The results will be presented in the next chapter.

CHAPTER 3 RESULTS AND DISCUSSION

3.1. Predicted vs. Experimental rocking natural frequency

There were two tests conducted to get the rocking natural frequency – the sweep test and the bump test. Both results will be compared to the predictions.

In the bump test, there was no test package. The only weight on the platform was a 5 pound steel block. Also, the number of support springs on each side was 2. In order to eliminate noise on the recorded waveform produced by the accelerometer mounted on the platform, the filter frequency was set to 5 times as the predicted rocking natural frequency. This is common practice in this field. The results of the bump test are shown in Table 3. The rocking frequency was measured from the decaying sine wave (Figure 29) and R was calculated from Equation (4).

Table 3 Rocking natural frequency and damping ratio from the bump test

Bumps	Filter Frequency (H_z)	Period (ms)	Bump Test_f_θ (H_z)	G_1	G_N	**R**
1 st	44	122	8.20	2.33	1.25	**0.03**
2 nd	44	124	8.06	2.18	1.02	**0.04**
3 rd	44	146	6.85	2.2	1.56	**0.02**
4 th	44	126	7.94	2	1.13	**0.03**
5 th	44	130	7.69	3.03	1.82	**0.03**

Figure 29 First bump test filtered at 44 Hz

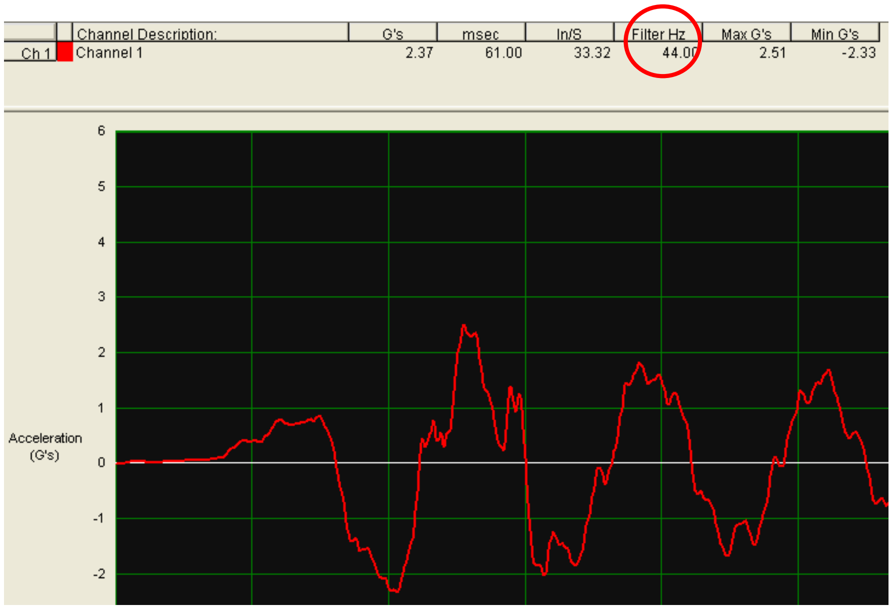

Different bumps produced different results for f_θ and R even though they were conducted under the same experiment conditions. The accelerometer is too sensitive, requiring filtering to eliminate noise, and the platform probably flexed, which could be reasons for this result.

Compare to the bump test, the sweep test results were much more repeatable. Table 4 shows the comparison between the predicted f_θ and the sweep test value. The sweep test value is the vibration table frequency that caused resonance. The predicted natural frequency was obtained from Equation (25) using the platform specifications in section 2.2.

Table 4 Prediction vs. experimental rocking natural frequency from the sweep test

Springs on each side / Mass weight (lbs.)	**Predicted f_θ (Hz)**	**Sweep Test f_θ (Hz)**	**Predicted f_θ (Hz)**	**Sweep Test f_θ (Hz)**	**Predicted f_θ (Hz)**	**Sweep Test f_θ (Hz)**
	2		**3**		**4**	
5	8.73	8.65	10.69	11.6	12.34	12
37	4.98	5.05	6.10	6.2	7.04	6.9
69	3.85	4.2	4.71	4.85	5.44	5.5
101.8	3.24	3.5	3.96	4	4.58	4.65

The good agreement between the predicted and experimental f_θ**'s s**hows that Equations (25) appear to be trustworthy.

3.2. Predicted RMS G

A series of vertical acceleration (G_z) samples were generated at 1 ms intervals and used as the trailer input G_{zt}. The vertical accelerations G_{zp} of a targeted position 30 inches from the centerline were then obtained to drive the vibration table.

For the prototype wooden platform, the spring constant (k) and the weight of the mass (M_m) are adjustable, while the locations of the springs and the mass are fixed (refer to Figure 26). In order to find the combinations of "k" and "M_m" that give the required $RMS\ G_{x,\,p}$, a program that uses the theoretical equations in Chapter 2 was written in Excel Macros (see Appendix A). For the targeted $RMS\ G_{x,\,p}$ = 0.0118 g's, all of the combinations of "k" and "M_m" that can produce this $RMS\ G_{x,\,p}$ are shown in Table 5. In this situation, the spring location (a) was 23 inches and mass location (X_m) was 20.5 inches.

Table 5 Predicted combinations of "k" and "M_m" that give target RMS

Number of springs	Spring constant (lb/in)	Weight of the mass (lbs.)	Simulated RMS G's
2	120	5	0.0109
3	180	5	0.0115
4	240	5	0.0119

The platform used in this research was a simplified version. As the locations of the springs and the mass were fixed, the mass needed to be removed to adjust the weight and/or springs needed to be taken out or added. This way is not very convenient for actual use. An easier adjustment for a commercial version of the platform is recommended. In the commercial version, only one set of springs and mass are needed and the locations of them ("a" and "X_m") become the variables. Adjustments can be made more easily by a crank handle as needed. Table 6 shows all combinations of "a" and "X_m" that could produce the same $RMS\ G_{x,\,p}$ as the simplified version based on the same input data. In this case, the spring constant (k) and the weight of the mass (M_m) were chosen to be 350 lb/in and 10 lbs, respectively. As a result, a wider range of RMS G's can be targeted because "a" and "X_m" can be adjusted continuously.

Table 6 Predicted combinations of "a" and "X_m" for the same target RMS $G_{x,P}$

Spring location away from axle (in)	Mass location away from axle (in)
3	7.84
4	6.38
5	6.49
6	6.7
7	6.15
8	5.74
9	5.77
10	5.93
11	5.97

Table 6 (cont'd)

12	6.11
13	6.31
14	6.47
15	6.63
16	6.84
17	7.12
18	7.47
20	8.29
21	8.74
22	9.21
23	9.7

The theoretical results in Table 5 show that it is possible to target a given lateral G_{xp} by using different combinations of spring constant and weight of the mass. An actual test was conducted to check if the predicted results could be verified. The input data was downloaded from a SAVER that was mounted on the A-frame of the platform. There were 3 springs supporting each side of the platform and one 5 pound weight was placed on it. The recorded vertical accelerations were used as the input G_{zp}, and then the angular acceleration $\ddot{\theta}$ and lateral acceleration G_{xp} were obtained through Equations (20) and (12). The RMS G from the recorded lateral accelerations was then compared with the one from the predicted lateral acceleration G_{xp}. See Table 7 for the result.

Table 7 Predicted and recorded RMS G's

Predicted lateral $RMS\ G_{xp}$	**Recorded lateral** $RMS\ G_{xp}$
0.139	1.2881

The result wasn't as good as expected. Even though the predicted and actual RMS G should be the same, there was a tenfold difference between them. They didn't match each other most likely because of the unwanted noise and vibration produced by the platform flexing and the axle wobbling. They were inferred from the signals the SAVER recorded.

Figure 30 shows the recorded lateral response. The SAVER recorded a constant frequency of 200 Hz with a peak acceleration up to 5 G’s. It can be inferred from the beat pattern that the A-frame and/or the platform were resonating.

Figure 30 Recorded acceleration in lateral direction

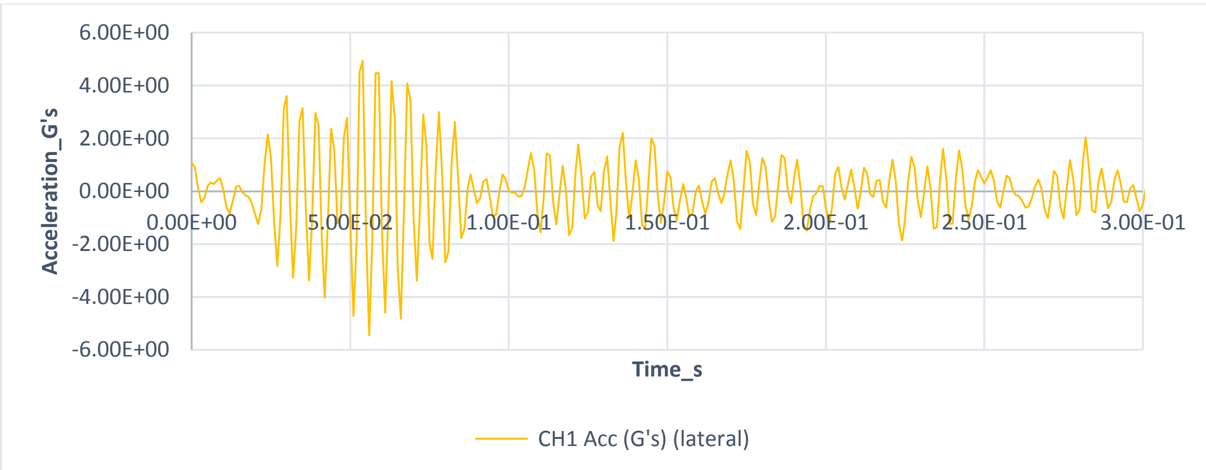

The recorded longitudinal accelerations (in the direction of the axle) are shown in Figure 31. Accelerations up to 2 G’s were recorded. They should be 0 G’s as there should be no vibration in this direction. The reason for this is that the platform was not stiff enough, especially the “A-frame”.

Figure 31 Recorded acceleration in longitudinal direction

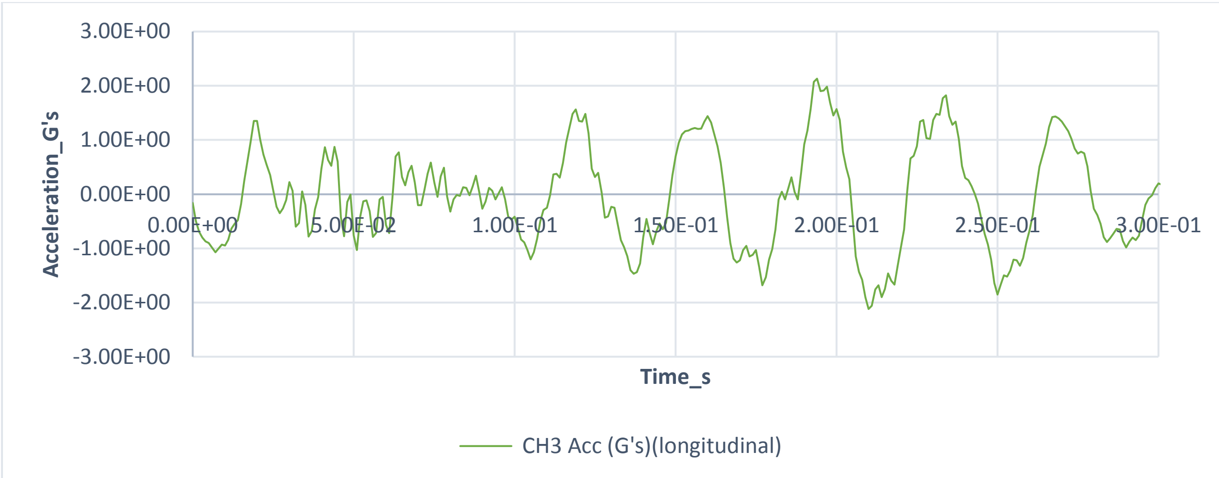

Additionally, the ASTM 4169 Truck II PSD spectrum (ASTM, 2005) was used to drive the table, which means the vertical accelerations SAVER recorded should be about 0.5 G's. Nevertheless, Figure 32 shows vertical accelerations as large as 3 G's. This was probably due to the axle being loose in the bearings, so unwanted noise and vibrations were produced.

Figure 32 Recorded acceleration in vertical direction

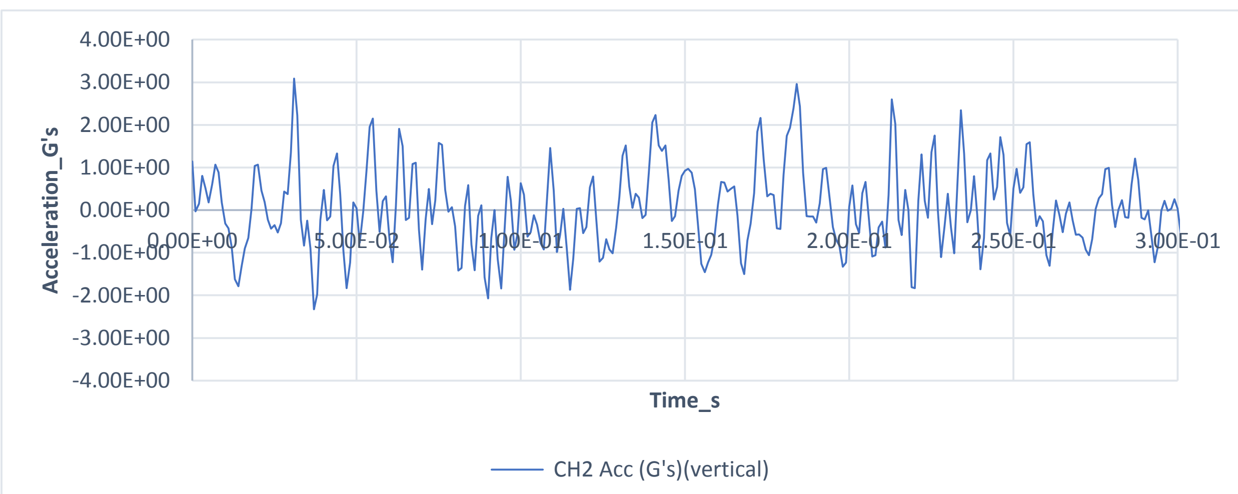

CHAPTER 4 CONCLUSIONS AND FUTURE WORK

For the reasons mentioned in Chapter 3, the predicted RMS G could not be verified using the experimental test results due to flexing of the platform and A-frame and rattling of the axle in the bearings. However, the predicted rocking natural frequency was verified using the sweep test, because this property doesn't depend on instantaneous accelerations. It is likely that we can trust the predicted RMS G even though the SAVER data does not confirm this.

If we want the vibration recorders to record noise free data, the platform should be built as stiff as possible with tight tolerances in the axle. This viewpoint is also a concern of the single-axis vibration table manufacture, Lansmont, in their instruction manual (Lansmont, 2011). Also, hard filtering acceleration data to remove unwanted platform vibrations will be helpful. This can be done by specifying some upper frequency cutoff and hard wiring a simple analog filter into the circuit.

In order to get the target $RMS\ G_{x,t}$ from the trailer, a multi-axis vibration recorder like the SAVER and its support frame will be needed. Lightweight beams as shown in Figure 22 should be used to build the frame.

In addition to rocking motion, this platform can also reproduce pitching motion, which happens when the front and back wheels of the trailer go over bumps at different times. As long as the beam attached to the trailer is parallel to the longitudinal direction, all the steps in section 4.1 can be repeated. As the length of a trailer is much larger than its width (40 feet vs. 8 feet), the angle of rotation caused by bumps or potholes will be about 5 times less than in the lateral direction, which is why pitching motion should not be considered.

4.1. Industry application of this research and matters that need attention

The following steps must be followed to use the platform to add rocking motion to a single-axis vertical vibration table:

a) Construct a lightweight beam like the one in Figure 22, making it as stiff as possible.

b) Mount a SAVER on the beam and attach the beam to the floor of a trailer. Mount this beam over one of the floor support beams if possible, refer to Figure 33 (Archer, June 2012). Make sure the SAVER is mounted on it midway between walls at a known height H_t (30 inches for example) above the trailer floor.

Figure 33 Bare chassis of a trailer showing support beams

c) Drive the trailer over the road that needs to be simulated and let the SAVER record the vertical and lateral accelerations (G_{zt} and G_{xt}) at 1 ms or 2 ms intervals.

d) Process the data from the SAVER through Equation (10) to get the vertical PSD plot ($RMS\ G_{z,\,p}$) at the target position P to be simulated. Follow the procedure in section 2.3.2.

e) Construct a rigid platform (refer to Figure 17) with an axle that fits tightly into bearings. Attach the bearings to the vibration table and add one spring (500 lbs./in would be a good start) on each side under the platform to support it.

f) Put a solid block (20 lbs. would be a good start) on one side of the platform and mounted a SAVER on the top of the A-frame (refer to Figure 24).

g) Place the test package on the center of the platform and secure it if necessary.

h) Run the vibration table with the target vertical PSD plot for position P and let the SAVER record the vibration in the vertical and lateral directions.

i) Download the SAVER data and compare the lateral RMS G with the predicted $RMS\ G_{x,\,p}$ in Equation (15).

j) Adjust the spring location (a) and the mass location (X_m) until the test result matches the prediction. Use the fact that the lateral RMS G will increase if the mass is moved further from the axle. It may both increase and decrease if the spring is moved further from the axle. The Table 8 and Figure 34 show the predicted trends.

Figure 8 Simulated RMS G's versus locations of the mass and the spring

Location of spring from axle (in)	**Location of mass from axle (in)**	**Simulated RMS G's**
2	6	0.0171
2	10	0.0269
2	14	0.0347
2	18	0.0403
6	6	0.0245

Table 8 (cont'd)

6	10	0.0372
6	14	0.0459
6	18	0.0517
10	6	0.0266
10	10	0.0421
10	14	0.0542
10	18	0.0622
14	6	0.0243
14	10	0.0386
14	14	0.0501
14	18	0.0584
18	6	0.0194
18	10	0.0315
18	14	0.0424
18	18	0.052
22	6	0.0156
22	10	0.0255
22	14	0.0345
22	18	0.0425

Figure 34 Plot of the relationship between RMS G and two variables

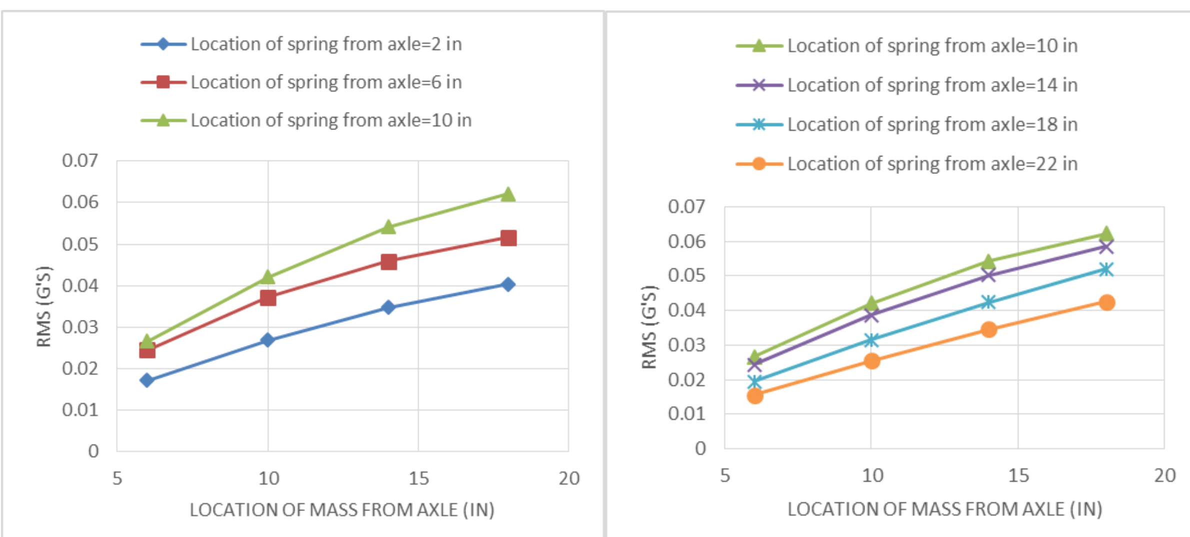

By trial and error, move the spring and the mass in small increments until the target $RMS\ G_{x,\,p}$ is reached, because the RMS G is sensitive to the locations of them, especially for the mass. Therefore, if the difference between target RMS G and tested result is big, adjusting the location of mass will hit the target quicker. Figure 34 also shows the adjustment of the spring is harder than the mass because the lateral RMS G will increase and decrease if increase the distance between the axle and the spring,

Another observation regarding the motion of platform deserves mentioning. At the moment when the vibration table was turned on, the vibration table surged upward. This is normal. When this happened, the platform rotated through a big angle. This suggests that vertical spikes are accompanied by rotational spikes. This also happens to the trailer floor when the trailer is over a pothole. This is confirmed by Equation (20). When there's a large input vertical acceleration G_{zp}, the angular acceleration $\ddot{\theta}$ will be large too.

There is always the possibility that the center of gravity (CG) of the system can be directly over the axle of the platform. This could happen if the test package has an irregular shape or is placed on the platform off center. In this case, the distance d from axle to system's CG will be zero, which makes C_3 in Equation (23) zero. Therefore, the angular acceleration in Equation (20) will be zero, which means the platform will only move up and down after the vibration table is turned on. In reality, the platform may rotate through a very small angle, but will be too small to be considered rocking vibration. When conducting the vibration test with the platform, people should pay attention to how to place the test package to avoid this situation. The system's CG should not be over the axle. Making sure that the platform rotates through some angle at rest prevents this.

4.2. Limitations of this research

a) Since the platform only has two parameters that can be adjusted to match rocking motion, the entire PSD plot cannot be reproduced by simply adjusting these limited variables. Instead, the area under the PSD plot (RMS G squared) was targeted to reproduce the lateral motion of the trailer. RMS G is the most important property of a PSD plot because it represents the overall severity of the ride.

b) This research focused on how to reproduce the rocking motion of the trailer floor. Both the test package and the platform are assumed to be solid masses. The predicted motion in section 2.3.3. was based on the assumption that the test package is a rigid mass, but actual packages do not always meet this criterion. If the package is flexible, its center of gravity will change because the product moves around inside the box. Therefore, the predicted RMS G will have some error. However, the space available for the product to move around inside the package is limited, so the location of the center of gravity won't change a lot. As a result, the predicted RMS G should not change very much.

c) Ideally, the platform should have the same decay rate as the trailers when bumped. This would require matching the damping motion and the RMS G at the same time. In order to match the damping motion of the trailer, the damping ratio R should be the same. Both can be obtained from a bump test. Mount a SAVER on the beam shown in Figure 35 (P. Singh, personal communication, 2006). Drive the trailer over a single bump (like over a curb) and get the decaying sine wave response from the SAVER. Analyze the response to get the rocking frequency and damping ratio through Equations (3)-(6) and then c will be obtained from Equation (21).

Figure 35 Location of the vibration recorder

The damping coefficient used for this research was obtained from the bump test on the platform, because this test is the only way to get it.

The damping coefficient c for the platform is determined by different kinds of friction, dry friction and viscous friction. There are two places where dry friction occurred. One is between the springs and the wooded pockets of the platform, because the spring is constantly rubbing against the wood during vibration. Another is between the axle and the bearings. This won't happen on a commercial platform because it will be built with ball bearings and there won't be any pockets for the springs. For viscous friction, there are two factors as well. One is the internal friction of the steel coils when the spring is compressed. The other is the air mass that must be moved during rocking. This provides resistance to the platform during vibration.

Since the adjustments to the platform are limited, the most important property of rocking motion should be matched with the trailer's, which is the lateral RMS G. The damping coefficient of the platform can be made to be adjustable by adding dampers to the platform. This will increase the damping coefficient.

d) The platform cannot simulate the motion of a trailer when it changes speed (surge), changes lanes (sway) and turns corners (yaw). These three motions are long duration events, lasting several seconds. The platform would have to move several feet to simulate this. Fortunately, these 3 motions only happen occasionally relative to vertical and rocking motion. In addition, they rarely provide enough power to affect the PSD plot, which is used to drive the vibration table. Multi-axis shakers have these same problems.

e) Even if the platform and its A-frame can be built as stiff as the vibration table itself, and with no noise coming from the axles, the simulated rocking motion will only get close to the real motion. In a trailer, there are 2 random inputs (left wheels and right wheels), while on a vibration table there is only 1 input. Therefore, there is no way to make the platform motion agree with trailer motion exactly.

4.3. Future work

First, a platform that is much stiffer must be built. The platform in this version should use the commercial design where the locations of the spring and the mass are variable. This new prototype should then be used to further verify the prediction model by comparing the lateral RMS G that SAVER measured with the one predicted by the model.

The next step would be to test actual packages on a trailer and on the platform. The actual package should be placed at whatever position on the trailer floor is to be simulated (position P). The vibration table should be driven with the PSD plot obtained through Equation (11). Either the program in Excel Macros or the trial and error approach above can be used to get the required information on how to set up the platform. The package tested on the platform should then be compared to the one tested on the trailer based on the damage they get. Consistency in damage levels will indicate how well the trailer movements are reproduced.

APPENDICES

Appendix A

Excel Macros for calculating “k”, “Mm” and “ $RMS\ G_{x,P}$ ” related to Table 5

```
Sub auto1()

Dim I As Integer

Dim Xm, Xg, Yg, Ip, Il, Im, MoI, Q, OMEGA As Variant

Dim C1, C2, C3, C4, C5, C6, C7, C8, C9, B1, B2, B3 As Variant

Dim SUMXT, SUMZT, SUMZP, DDX0, DDX1, DDXT, DDXT0, DDXT1, DDZT0,
DDZT1, DDZT, DDZP, TH, TH1, DTH, DTH1, DDTH, AVG, DDTHETA, DDX, SUM
As Variant

'trailer Gz & Gx and target platform rms

N = 3500: G = 386.4: T = 0.001

HTR = 36 'height of trailer saver above floor

SUMXT = 0: SUMZT = 0 : C = 5

For I = 1 To N

DDXT = Sheet1.Cells(I, "A").Value : DDZT = Sheet1.Cells(I, "B").Value

SUMXT = (DDXT) ^ 2 + SUMXT : SUMZT = (DDZT) ^ 2 + SUMZT

Next I

RMSXT = Sqr(SUMXT / N) : RMSZT = Sqr(SUMZT / N)

Sheet1.Cells(1, "D").Value = "trailer: lateral Grms= " & Round(RMSXT, 8)

Sheet1.Cells(2, "D").Value = "trailer: vertical Grms= " & Round(RMSZT, 8)

D = 30 'location on trailer floor to simulate - distance from centerline

HPL = 15 ' height of saver above axle on platform

SUMZP = 0

For I = 1 To N

DDXT = Sheet1.Cells(I, "A").Value : DDZT = Sheet1.Cells(I, "B").Value

DDTHETA = -DDXT * G / HTR 'target position's angular acc's

DDZP = DDZT + D * DDTHETA / G 'target position's vertical acc's/axle gz

SUMZP = SUMZP + (DDZP) ^ 2

Next I

RMSZP = Sqr(SUMZP / N)
```

```
RMSXP = (HPL / HTR) * RMSXT 'taget rms - rmsxp
Sheet1.Cells(1, "E").Value = "platform: lateral Grms= " & Round(RMSXP, 8)
Sheet1.Cells(2, "E").Value = "platform: vertical Grms= " & Round(RMSZP, 8)
'platform settings
Mp = 40 / G: Lp = 48: Hp = 6: Xp = 0: Yp = 0
Ml = 48 / G: Ll = 12: Hl = 36: Xl = 0: Yl = 18
                Lm = 6.75: Hm = 2: Ym = 4: Xm = 20.5
IJ = 2 : A = 23 'location of the springs
For K = 60 To 240 Step 60 'spring costant
For Mm = 5/G To 101.8/G Step 5/G 'weight of the mass
Mass = Mp + Ml + Mm
   Xg = (Mp * Xp + Ml * Xl + Mm * Xm) / Mass
   Yg = (Mp * Yp + Ml * Yl + Mm * Ym) / Mass
   Ip = Mp * ((Lp) ^ 2 + (Hp) ^ 2) / 12 + Mp * ((Xp - Xg) ^ 2 + (Yp - Yg) ^ 2)
   Il = Ml * ((Ll) ^ 2 + (Hl) ^ 2) / 12 + Ml * ((Xl - Xg) ^ 2 + (Yl - Yg) ^ 2)
   Im = Mm * ((Lm) ^ 2 + (Hm) ^ 2) / 12 + Mm * ((Xm - Xg) ^ 2 + (Ym - Yg) ^ 2)
   MoI = Ip + Il + Im : Q = MoI + Mass * (Xg) ^ 2
   C1 = C * (A) ^ 2 / Q: C2 = K * (A) ^ 2 / Q: C3 = -Mass * Xg / Q
   OMEGA = Sqr(C2 - (C1) ^ 2 / 4)
   B1 = Exp(-C1 * T / 2): B2 = Sin(OMEGA * T): B3 = Cos(OMEGA * T)
TH = 0: DTH = 0
DDXT00 = Sheet1.Cells(1, "A").Value : DDZT00 = Sheet1.Cells(1, "B").Value
DDTHETA00 = -DDXT00 * G / HTR
DDZP00 = DDZT00 + D * DDTHETA00 / G
SUM = (HPL * C3 * DDZP00) ^ 2
For J = 1 To N - 1
      DDXT0 = Sheet1.Cells(J, "A").Value
      DDZT0 = Sheet1.Cells(J, "B").Value
      DDTHETA0 = -DDXT0 * G / HTR
      DDZP0 = DDZT0 + D * DDTHETA0 / G
```

```
        DDXT1 = Sheet1.Cells(J + 1, "A").Value
        DDZT1 = Sheet1.Cells(J + 1, "B").Value
        DDTHETA1 = -DDXT1 * G / HTR
        DDZP1 = DDZT1 + D * DDTHETA1 / G
        C6 = DDZP0 * G: C7 = (DDZP1 - DDZP0) * G / T
        C9 = C3 * C7 / C2: C8 = (C3 * C6 - C1 * C9) / C2
        C5 = TH - C8: C4 = (DTH + C1 * C5 / 2 - C9) / OMEGA
        TH1 = B1 * (C4 * B2 + C5 * B3) + C8 + C9 * T
        DTH1 = B1 * (-(OMEGA * C5 + C1 * C4 / 2) * B2 + (OMEGA * C4 - C1 * C5 / 2)
* B3) + C9
        DDTH = C3 * DDZP1 * G - C1 * DTH1 - C2 * TH1
        DDX = HPL * DDTH / G
        SUM = SUM + (DDX) ^ 2
        DTH = DTH1 : TH = TH1
Next J
    RMS = Sqr(SUM / N)
    If Abs(RMS - RMSXP) < 0.001 Then
    Sheet1.Cells(IJ, "F") = K : Sheet1.Cells(IJ, "G") = M
    Sheet1.Cells(IJ, "H") = Round(RMS, 4)
    IJ = IJ + 1
    End If
    Next M
    Next K
    Sheet1.Cells(1, "F") = "Spring constant on each side_lb/in"
    Sheet1.Cells(1, "G") = "Weight of the mass_lbs."
    Sheet1.Cells(1, "H") = "Simulated RMS G's"
    Sheet1.Cells(1, "I") = "Difference between simulated and target RMS G's"
End Sub
```

Appendix B

Excel Macros for calculating “a” and “Xm” related to Table 6

```
Sub auto2()

Dim I As Integer

Dim Xm, Xg, Yg, Ip, Il, Im, MoI, Q, OMEGA As Variant

Dim C1, C2, C3, C4, C5, C6, C7, C8, C9, B1, B2, B3 As Variant

Dim SUMXT, SUMZT, SUMZP, DDX0, DDX1, DDXT, DDXT0, DDXT1, DDZT0,
DDZT1, DDZT, DDZP, TH, TH1, DTH, DTH1, DDTH, AVG, DDTHETA, DDX, SUM
As Variant

'trailer Gz & Gx and target platform rms

N = 3500: G = 386.4: T = 0.001 : K = 350: C = 5

HTR = 36 'height of trailer saver above floor

SUMXT = 0: SUMZT = 0

For I = 1 To N

DDXT = Sheet1.Cells(I, "A").Value : DDZT = Sheet1.Cells(I, "B").Value

SUMXT = (DDXT) ^ 2 + SUMXT : SUMZT = (DDZT) ^ 2 + SUMZT

Next I

RMSXT = Sqr(SUMXT / N) : RMSZT = Sqr(SUMZT / N)

Sheet1.Cells(1, "D").Value = "trailer: lateral Grms= " & RMSXT

Sheet1.Cells(2, "D").Value = "trailer: vertical Grms= " & RMSZT

D = 30 'location on trailer floor to simulate - distance from centerline

HPL = 15 'height of saver above axle on platform

SUMZP = 0

For I = 1 To N

DDXT = Sheet1.Cells(I, "A").Value : DDZT = Sheet1.Cells(I, "B").Value

DDTHETA = -DDXT * G / HTR 'target position's angular acc's

DDZP = DDZT + D * DDTHETA / G 'target position's vertical acc's/axle gz

SUMZP = SUMZP + (DDZP) ^ 2

Next I

RMSZP = Sqr(SUMZP / N)
```

```
RMSXP = (HPL / HTR) * RMSXT 'taget rms - rmsxp
Sheet1.Cells(1, "E").Value = "platform: lateral Grms= " & RMSXP
Sheet1.Cells(2, "E").Value = "platform: vertical Grms= " & RMSZP
'default settings
Mp = 40 / G: Lp = 48: Hp = 6: Xp = 0: Yp = 0
Ml = 48 / G: Ll = 12: Hl = 36: Xl = 0: Yl = 18
Mm = 10 / G: Lm = 8: Hm = 2: Ym = 4
Mass = Mp + Ml + Mm : IJ = 2
For A = 3 To 23 Step 1 'location of the spring
LOW = 6: HIGH = 20: DXM = 1
3   For Xm = LOW To HIGH Step DXM 'locaiton of the mass
    Xg = (Mp * Xp + Ml * Xl + Mm * Xm) / Mass
    Yg = (Mp * Yp + Ml * Yl + Mm * Ym) / Mass
    Ip = Mp * ((Lp) ^ 2 + (Hp) ^ 2) / 12 + Mp * ((Xp - Xg) ^ 2 + (Yp - Yg) ^ 2)
    Il = Ml * ((Ll) ^ 2 + (Hl) ^ 2) / 12 + Ml * ((Xl - Xg) ^ 2 + (Yl - Yg) ^ 2)
    Im = Mm * ((Lm) ^ 2 + (Hm) ^ 2) / 12 + Mm * ((Xm - Xg) ^ 2 + (Ym - Yg) ^ 2)
    MoI = Ip + Il + Im : Q = MoI + Mass * (Xg) ^ 2
    C1 = C * (A) ^ 2 / Q: C2 = K * (A) ^ 2 / Q: C3 = -Mass * Xg / Q
    OMEGA = Sqr(C2 - (C1) ^ 2 / 4)
    B1 = Exp(-C1 * T / 2): B2 = Sin(OMEGA * T): B3 = Cos(OMEGA * T)
TH = 0: DTH = 0
DDXT00 = Sheet1.Cells(1, "A").Value : DDZT00 = Sheet1.Cells(1, "B").Value
DDTHETA00 = -DDXT00 * G / HTR
DDZP00 = DDZT00 + D * DDTHETA00 / G
SUM = (HPL * C3 * DDZP00) ^ 2
For J = 1 To N - 1
        DDXT0 = Sheet1.Cells(J, "A").Value : DDZT0 = Sheet1.Cells(J, "B").Value
        DDTHETA0 = -DDXT0 * G / HTR
        DDZP0 = DDZT0 + D * DDTHETA0 / G
        DDXT1 = Sheet1.Cells(J + 1, "A").Value
```

```
        DDZT1 = Sheet1.Cells(J + 1, "B").Value
        DDTHETA1 = -DDXT1 * G / HTR
        DDZP1 = DDZT1 + D * DDTHETA1 / G
        C6 = DDZP0 * G: C7 = (DDZP1 - DDZP0) * G / T
        C9 = C3 * C7 / C2: C8 = (C3 * C6 - C1 * C9) / C2
        C5 = TH - C8: C4 = (DTH + C1 * C5 / 2 - C9) / OMEGA
        TH1 = B1 * (C4 * B2 + C5 * B3) + C8 + C9 * T
        DTH1 = B1 * (-(OMEGA * C5 + C1 * C4 / 2) * B2 + (OMEGA * C4 - C1 * C5 / 2)
* B3) + C9
        DDTH = C3 * DDZP1 * G - C1 * DTH1 - C2 * TH1
        DDX = HPL * DDTH / G
       SUM = SUM + (DDX) ^ 2
        DTH = DTH1 : TH = TH1
Next J
    RMS = Sqr(SUM / N)
    If RMS < RMSXP Then GoTo 1
    LOW = Xm - DXM: HIGH = Xm: DXM = DXM / 10
    If DXM < 0.00001 Then
    Sheet1.Cells(IJ, "F") = A
    Sheet1.Cells(IJ, "G") = Round(Xm, 2)
    IJ = IJ + 1
    GoTo 2
    End If
    GoTo 3
1   Next Xm
2 Next A
    Sheet1.Cells(1, "F") = "SPRING'S LOCATION AWAY FROM AXLE_in"
    Sheet1.Cells(1, "G") = "MASS'S LOCATION AWAY FROM AXLE_in"
   End Sub
```

Appendix C

Excel Macros for predicted and experimental "$RMS\ G_{x,P}$" related to Table 7

```
Sub rmsmeasuredandcalculated()

Dim Gz0, Gz1, Gr1, C4, C5, C6, C7, C8, C9, TH1, DTH1, DDTH, DTH, TH, SUMR1,
SUMX1 As Variant

N = 2048

K = 180: C = 5: T = 0.001: G = 386.4: HPL = 15: A = 23

SUMX1 = 0: SUMR1 = 0

Mp = 40 / G: Lp = 48: Hp = 6: Xp = 0: Yp = 0

Mm = 5 / G: Lm = 6: Hm = 0.5: Ym = 3.25: Xm = 20.5

Mass = Mp + Mm

   Xg = (Mp * Xp + Mm * Xm) / Mass

   Yg = (Mp * Yp + Mm * Ym) / Mass

   Ip = Mp * ((Lp) ^ 2 + (Hp) ^ 2) / 12 + Mp * ((Xp - Xg) ^ 2 + (Yp - Yg) ^ 2)

   Im = Mm * ((Lm) ^ 2 + (Hm) ^ 2) / 12 + Mm * ((Xm - Xg) ^ 2 + (Ym - Yg) ^ 2)

   MoI = Ip + Im : Q = MoI + Mass * (Xg) ^ 2

   C1 = C * (A) ^ 2 / Q: C2 = K * (A) ^ 2 / Q: C3 = -Mass * Xg / Q

   OMEGA = Sqr(C2 - (C1) ^ 2 / 4)

   B1 = Exp(-C1 * T / 2): B2 = Sin(OMEGA * T): B3 = Cos(OMEGA * T)

TH = 0: DTH = 0

Gz010 = Sheet1.Cells(2, "C").Value

SUMX2 = (HPL * C3 * Gz010) ^ 2

For I = 2 To N

Gz01 = Sheet1.Cells(I, "C").Value

Gz11 = Sheet1.Cells(I + 1, "C").Value

C6 = Gz0 * G: C7 = (Gz11 - Gz01) * G / T

C9 = C3 * C7 / C2: C8 = (C3 * C6 - C1 * C9) / C2

C5 = TH - C8: C4 = (DTH + C1 * C5 / 2 - C9) / OMEGA

TH1 = B1 * (C4 * B2 + C5 * B3) + C8 + C9 * T
```

```
DTH1 = B1 * (-(OMEGA * C5 + C1 * C4 / 2) * B2 + (OMEGA * C4 - C1 * C5 / 2) *
B3) + C9

DDTH = C3 * Gz11 * G - C1 * DTH1 - C2 * TH1

DDX = HPL * DDTH / G

SUMX1 = SUMX1 + (DDX) ^ 2 ‘predicted RMS G

DTH = DTH1

TH = TH1

Next I

For J = 2 To N + 1

Gr1 = Sheet1.Cells(J, "B").Value

SUMR1 = SUMR1 + (Gr1) ^ 2 ‘recorded RMS G

Next J

RMSx1 = Sqr(SUMX1 / N)

RMSr1 = Sqr(SUMR1 / N)

Sheet1.Cells(2, "F").Value = "Predicted lateral RMS= " & Round(RMSx1, 4)

Sheet1.Cells(3, "F").Value = "Recorded lateral RMS= " & Round(RMSr1, 4)

End Sub
```

Appendix D

Excel Macros for "$RMS\ G_{x,P}$" vs. "a" and "Xm" related to Table 8

```
Sub variousRMS3GB()

Dim I As Integer

Dim Gx, Gz, DDTHETA, Gzp As Variant

Dim MM, MASS, XG, YG, IP, IM, IL, MOI, Q, C1, C2, C3, R, OMEG As Variant

Dim TH, DTH, SUM, Gz0, Gx0, Gz1, Gx1, DDTHETA0, DDTHETA1, Gzp0, Gzp1 As
Variant

Dim C6, C7, C9, C8, C5, C4, Z1, Z2, Z3, DDTH, Gxp As Variant

D = 30: HTR = 36: HPL = 15: N = 3500: T = 0.001: G = 386.4

C = 5: J = 2: K = 500 'spring constant

MP = 40 / G: LP = 48: HP = 6: XP = 0: YP = 0

MM = 20 / G: LM = 8: HM = 2: YM = 4: 'Xm = 20

ML = 48 / G: LL = 12: HL = 36: XL = 0: YL = 18

MASS = MP + MM + ML

For A = 2 To 23 Step 4 'location of the spring

  For Xm = 6 To 20 Step 4 'location of the mass

  XG = (MP * XP + MM * Xm + ML * XL) / MASS

  YG = (MP * YP + MM * YM + ML * YL) / MASS

  IP = MP * ((LP) ^ 2 + (HP) ^ 2) / 12 + MP * ((XP - XG) ^ 2 + (YP - YG) ^ 2)

  IM = MM * ((LM) ^ 2 + (HM) ^ 2) / 12 + MM * ((Xm - XG) ^ 2 + (YM - YG) ^ 2)

  IL = ML * ((LL) ^ 2 + (HL) ^ 2) / 12 + ML * ((XL - XG) ^ 2 + (YL - YG) ^ 2)

  MOI = IP + IM + IL: Q = MOI + MASS * (XG) ^ 2

  C1 = C * (A) ^ 2 / Q: C2 = K * (A) ^ 2 / Q: C3 = -MASS * XG / Q

  R = C1 / 2 / Sqr(C2): OMEG = Sqr(C2 * (1 - (R) ^ 2))

  TH = 0: DTH = 0

  Gx00 = Sheet3.Cells(1, "a").Value

  Gz00 = Sheet3.Cells(1, "b").Value

  DDTHETA00 = -Gx00 * G / HTR

  Gzp00 = Gz00 + D * DDTHETA00 / G
```

```
    SUM = (HPL * C3 * Gzp00) ^ 2
        For I = 1 To N - 1
        Gx0 = Sheet3.Cells(I, "a").Value: Gx1 = Sheet3.Cells(I + 1, "a").Value
        Gz0 = Sheet3.Cells(I, "b").Value: Gz1 = Sheet3.Cells(I + 1, "b").Value
        DDTHETA0 = -Gx0 * G / HTR: DDTHETA1 = -Gx1 * G / HTR
        Gzp0 = Gz0 + D * DDTHETA0 / G: Gzp1 = Gz1 + D * DDTHETA1 / G
        C6 = Gzp0 * G: C7 = (Gzp1 - Gzp0) * G / T
        C9 = C3 * C7 / C2: C8 = (C3 * C6 - C1 * C9) / C2
        C5 = TH - C8: C4 = (DTH + C1 * C5 / 2 - C9) / OMEG
        Z1 = Exp(-C1 * T / 2): Z2 = Sin(OMEG * T): Z3 = Cos(OMEG * T)
        TH = Z1 * (C4 * Z2 + C5 * Z3) + C8 + C9 * T
        DTH = Z1 * (-(OMEG * C5 + C1 * C4 / 2) * Z2 + (OMEG * C4 - C1 * C5 / 2) *
Z3) + C9
        DDTH = C3 * Gzp1 * G - C1 * DTH - C2 * TH
        Gxp = HPL * DDTH / G
        SUM = SUM + (Gxp) ^ 2
        Next I
    RMS = Sqr(SUM / N)
    Sheet3.Cells(J, "D").Value = A
    Sheet3.Cells(J, "E").Value = Xm
    Sheet3.Cells(J, "F").Value = Round(RMS, 4)
    J = J + 1
    Next Xm
Next A
End Sub
```

REFERENCES

REFERENCES

Archer, R. (June 2012). Robert Archer Collection. Retrieved from http://www.hankstruckpictures.com/pix/trucks/archer/2012/06-24/bare_chassis_b_train_6-23-12.jpg

ASTM. (2005). Standard Practice for Performance Testing of Shipping Containers and Systems *D4169-05*: ASTM international.

ASTM. (2012). Standard Test Method for Random Vibration Testing of Shipping Containers *D4728 - 06*: ASTM International

ASTM. (2015). Standard Test Methods for Vibration Testing of Shipping Containers *D999 - 08*: ASTM International

Bernad, C., Laspalas, A., González, D., Liarte, E., & Jiménez, M. A. (2010). Dynamic study of stacked packaging units by operational modal analysis. *Packaging Technology and Science*, n/a-n/a. doi:10.1002/pts.883

Bernad, C., Laspalas, A., González, D., Núñez, J. L., & Buil, F. (2011). Transport vibration laboratory simulation: On the necessity of multiaxis testing. *Packaging Technology and Science, 24*(1), 1-14. doi:10.1002/pts.913

Burgess, G. (2013). Vibration Background/Case Studies [Class handout]. School of Packaging, Michigan State University, E Lansing, MI.

FedEx. (2011). Testing Packaged Products Weighing up to 150 Lbs. Retrieved from http://images.fedex.com/us/services/pdf/PKG_Testing_Under150Lbs.pdf

Lansmont. (2010). Model 7000 Vibration Test System. Retrieved from http://www.lansmont.com/products/vibration/vertical/lansmont-standard-7200/

Lansmont. (2011). Lansmont_Field-to-Lab®. Retrieved from http://www.lansmont.dk/images/Lansmont_Catalog-1.pdf

Lansmont. (2012, 3.8). Mechanical Shaker. Retrieved from http://cdn2.hubspot.net/hub/409629/file-1616859897-pdf/eBooks/Spec_Sheets/Mechanical_Shaker/Lansmont_Mechanical_Shaker.pdf

Lansmont. (2014, 10.2). CUBE™ Vibraiton Tester. Retrieved from http://cdn2.hubspot.net/hub/409629/file-1764455013-pdf/eBooks/Spec_Sheets/Vibration/Lansmont_Vibration_CUBE_10_14.pdf

Peterson, C. (2013). Time-to-Failure Testing Using Single- and Multi-Axis Vibration. *Sound and Vibration, 47*(3), 13-16. Retrieved from <Go to ISI>://WOS:000341446100003

Rouillard, V. (2013). *Some Observations on the Heave, Pitch and Roll Vibration of Road Transport Vehicles*. Paper presented at the ISTA TransPack Forum.

Shabana, A. A. (1995). *Theory of Vibration: An Introduction*: Springer New York.

Singh, P., Antle, J., & Burgess, G. (1992). Comparison between lateral, longitudinal, and vertical vibration levels in commercial truck shipments. *Packaging Technology and Science, 5*, 71-75.

W.B. Jones Spring Co., I. Compression Spring - P/N C48-187-192. Retrieved from http://www.springsfast.com/part_detail_compression.php?part=C48-187-192